Cholangiopathy aggravation is caused by VDR ablation and alleviated by VDR-independent vitamin D signaling in ABCB4 knockout mice

Ester Gonzalez-Sanchez, Haquima El Mourabit, Marion Jager, Marie Clavel, Sophie Moog, Javier Vaquero, Tatiana Ledent, Axelle Cadoret, Jérémie Gautheron, Laura Fouassier, et al.

HAL Id: hal-03971585

https://hal.sorbonne-universite.fr/hal-03971585v1

Submitted on 8 Feb 2023 (v1), last revised 6 Feb 2023 (v2)

Cholangiopathy aggravation is caused by VDR ablation and alleviated by VDR-independent vitamin D signaling in ABCB4 knockout mice

Ester Gonzalez-Sanchez [a,b,c,*,1], Haquima El Mourabit [a], Marion Jager [a], Marie Clavel [a,b], Sophie Moog [a,b], Javier Vaquero [a,c,d,1], Tatiana Ledent [a], Axelle Cadoret [a], Jérémie Gautheron [a], Laura Fouassier [a], Dominique Wendum [a,e], Nicolas Chignard [b,#], Chantal Housset [a, f,*,#]

[a]Sorbonne Université, INSERM, Centre de Recherche Saint-Antoine (CRSA), Paris, France;

[b]Inovarion, Paris, France;

[c]Oncology Program, CIBEREHD, National Biomedical Research Institute on Liver and Gastrointestinal Diseases, Instituto de Salud Carlos III, Madrid, Spain; TGF-β and Cancer Group, Oncobell Program, Bellvitge Biomedical Research Institute (IDIBELL), Barcelona, Spain;

[d] LPP (Laboratoire de physique des plasmas, UMR 7648), Sorbonne Université, Centre national de la recherche scientifique (CNRS), Ecole Polytechnique, 75005 Paris, France;

[e]Assistance Publique-Hôpitaux de Paris (AP-HP) Sorbonne Université, Hôpital St Antoine, Paris, France;

[f]AP-HP, Reference Center for Inflammatory Biliary Diseases and Autoimmune Hepatitis (CRMR, MIVB-H), Department of Hepatology, Saint-Antoine Hospital, Paris, France.

Ester Gonzalez-Sanchez (ester.glezsan@gmail.com), Haquima El Mourabit (haquima.el-mourabit@inserm.fr), Marion Jager (marion.jager@hotmail.fr), Marie Clavel (marie.clavel@inovarion.com), Sophie Moog (sophie.moog@inovarion.com), Javier Vaquero (jvaquero@idibell.cat), Tatiana Ledent (tatiana.ledent@gmail.com), Axelle Cadoret (axelle.cadoret@inserm.fr), Jérémie Gautheron (jeremie.gautheron@inserm.fr), Laura Fouassier (laura.fouassier@inserm.fr), Dominique Wendum (dominique.wendum@aphp.fr), Nicolas Chignard (nicolas.chignard@inovarion.com), Chantal Housset (chantal.housset@inserm.fr).

*Corresponding authors:

Chantal Housset, M.D., Ph.D.

Sorbonne Université, Faculté de Médecine, Site Saint-Antoine, 27 rue Chaligny, 75571 Paris cedex 12, France. E-mail: chantal.housset@inserm.fr; Phone: (33) 1-40-01-13-59

Ester Gonzalez-Sanchez, Ph.D.
TGF-Beta and Cancer Group, IDIBELL,Gran Via de L'Hospitalet, 199, 08908 Barcelona, Spain. E-mail: ester.glezsan@gmail.com; Phone: (34) 932607429

#These authors share senior authorship

1Ester Gonzalez-Sanchez and Javier Vaquero are currently affiliated to Oncology Program, CIBEREHD, National Biomedical Research Institute on Liver and Gastrointestinal Diseases, Instituto de Salud Carlos III, Madrid, Spain; TGF-β and Cancer Group, Oncobell Program, Bellvitge Biomedical Research Institute (IDIBELL), Barcelona, Spain.

Abbreviations: ABCB4, ATP-binding cassette transporter B4; PSC, primary sclerosing cholangitis; VDR, vitamin D receptor; PDIA3, protein disulfide-isomerase A3; ERp57, endoplasmic reticulum protein 57; IPSCSG, International Primary Sclerosing Cholangitis Study Group; AST, aspartate aminotransferase; ALP, alkaline phosphatase; CK19, cytokeratin 19; TNFα, tumor necrosis factor α; HPRT1, hypoxanthine phosphoribosyltransferase 1; GAPDH, glyceraldehyde 3-phosphate dehydrogenase; VCAM1, vascular cell adhesion molecule 1; CCL, C-C motif chemokine ligand; MMP9, matrix metalloproteinase 9; CCR, C-C motif chemokine receptor.

ABSTRACT

Background & Aims: Cholangiopathies are chronic liver diseases in which damaged cholangiocytes trigger a proinflammatory and profibrotic reaction. The nuclear vitamin D receptor (VDR) is highly expressed in cholangiocytes and exerts immune-regulatory functions in these cells. In the present study, we examined the protective function of VDR and other vitamin D signaling pathways in chronic cholangiopathy and cholangiocytes.

Methods: *Vdr* was invalidated in *Abcb4* knockout mice, a widely used animal model of chronic cholangiopathy. The impact of vitamin D signaling on cholangiopathy features was examined *in vivo* and in cholangiocytes (primary and cell lines).

Results: Cholangiopathy features (*i.e*, cholestasis, ductular reaction and fibrosis) were aggravated in *Vdr;Abcb4* double knockout mice compared to the *Abcb4* simple knockout, and associated with an overexpression of proinflammatory factors. The proinflammatory phenotype of cholangiocytes was also exacerbated following VDR silencing *in vitro*. The expression of proinflammatory factors and the severity of cholangiopathy were reduced in the double knockout mice treated with the vitamin D analog calcipotriol or with vitamin D. *In vitro*, the inflammatory response to TNFα was significantly reduced by calcipotriol in biliary cells silenced for VDR, and this effect was abolished by co-silencing the plasma membrane receptor of vitamin D, protein disulfide-isomerase A3 (PDIA3).

Conclusions: Our results demonstrate an anti-inflammatory role of VDR signaling in cholangiocytes and cholangiopathy. They also provide evidence for PDIA3-mediated anti-inflammatory effects of vitamin D and vitamin D analog in these settings.

Keywords: Cholangiocyte; Cholestasis; Ductular reaction; Liver fibrosis; Protein disulfide-isomerase A3.

1. INTRODUCTION

Cholangiopathies are chronic liver diseases in which damaged cholangiocytes trigger a proinflammatory and profibrotic response, that leads to the development of cirrhosis and end-stage liver disease [1]. Vitamin D deficiency is common in chronic liver diseases, and it is associated with increased liver inflammation and fibrosis [2-5]. It has also been reported that vitamin D deficiency is associated with an aggravation of liver fibrosis in a model of chronic cholangiopathy [6] that mimics primary sclerosing cholangitis (PSC), *i.e.*, the ATP-binding cassette transporter B4 (*Abcb4*) knockout mouse model [7-10]. Currently there are two vitamin D receptors described to mediate the biological effects of vitamin D. The nuclear receptor, vitamin D receptor (VDR), is the best characterized of these receptors. A membrane-associated receptor of vitamin D, protein disulfide-isomerase A3 (PDIA3) also known as endoplasmic reticulum protein 57 (ERp57), has also been described [11]. While PDIA3 elicits non-genomic responses, VDR mediates the biological effects of vitamin D by modulating the transcription of target genes. Especially, VDR mediates anti-inflammatory and anti-fibrotic effects of vitamin D through gene regulation. Of particular interest with respect to cholangiopathies, VDR expression is restricted to non-parenchymal cells in the liver, and largely predominant in cholangiocytes [12, 13], implying direct actions of VDR in cholangiocytes and cholangiopathies. Furthermore, VDR gene variations have been associated with auto-immune biliary diseases [14]. We previously showed that VDR promoted innate immunity in cholangiocytes [15] and that the absence of VDR altered the biliary epithelial cell barrier function leading to an aggravated phenotype of acute cholestatic liver injury in the mouse model of bile duct ligation [16]. We also showed that VDR expression in cholangiocytes was increased in the *Abcb4* knockout mice [13], suggesting an activation

of VDR signaling in a chronic setting of cholangiopathy. Moreover, other ligands such as bile acids may account for VDR protective effects in the liver [15].

In the present study we tested the protective function of VDR in chronic cholangiopathy by inactivating VDR in the *Abcb4* knockout mouse model and we also evaluated the potential of vitamin D and vitamin D analog to exert VDR-independent effects in this model and in cholangiocyte cell models.

2. MATHERIALS AND METHODS

2.1. Animal experiments

Abcb4 simple knockout mice and their wildtype littermates were bred, using *Abcb4*$^{+/-}$ heterozygous mice on an FVB/N genetic background (FVB.129P2-Abcb4tm1Bor/J) provided by Sanofi R&D (Chilly-Mazarin, France). To develop *Vdr*;*Abcb4* double knockout congenic mice, first we generated *Vdr*$^{+/-}$ mice on an FVB/N background. *Vdr*$^{+/-}$ mice on a C57BL/6J background (B6.129S4-Vdr^{tm1Mbd}/J) from Charles River Laboratories (Wilmington, MA, USA), were backcrossed with wildtype FVB/N mice (Charles River Laboratories) for 5 generations, using a speed congenics protocol. Next, *Vdr*$^{+/-}$ and *Abcb4*$^{-/-}$ mice on a FVB/N background were crossed to generate *Vdr*$^{+/-}$;*Abcb4*$^{-/-}$ mice, which were further crossed to obtain *Vdr*$^{+/+}$;*Abcb4*$^{-/-}$ and *Vdr*$^{-/-}$;*Abcb4*$^{-/-}$ mice (Supplementary Figure S1 A-B). Wildtype mice used as a reference in the study, were all on a FVB/N background. Mice were housed at CRSA animal facility (Institutional Animal Care and Use Direction, DDPP agreement No. C 75-12-01), in a temperature-controlled, specific pathogen-free environment, on a 12-hour light-dark cycle, with free access to a standard chow containing 1.2 IU vitamin D/kg (LASQCdiet® Rod16-R, Genobios, Laval, France) and water. All investigations were performed in males. During housing, animals were monitored daily for healthy status. Sub-groups of mice received intraperitoneal injections of 40 µg/kg calcipotriol (Tocris, Bristol, UK), 3 times a week, an optimal dose to produce beneficial effects according to a previous report [17], from the age of 4 weeks to 8 weeks, or long-term vitamin D dietary supply, in which case, mice were fed a diet containing 2.2 IU vitamin D/kg, enriched in calcium and phosphate (TD96348, Envigo, Huntington, UK) [16] after weaning at 4 weeks, until the

age of 12 months. Mice were included in lifespan studies or sacrificed under isoflurane anesthesia, at different time points. Upon sacrifice, blood was withdrawn from the vena cava and the liver and spleen were collected and weighed. Liver samples were harvested following recommendations from the International Primary Sclerosing Cholangitis Study Group (IPSCSG) [10]. In a sub-set of experiments, cholangiocytes and different liver cell types were isolated from 8 week-old mice, using an *in situ* perfusion-based protocol, as previously described [13]. All experiments complied with the European Directive 2010/63/UE and the ARRIVE Guidelines, and were approved by the Ethics Committee of Animal Experiments, Charles Darwin No.5 (No. APAFIS#364-2015032410575237v3 and APAFIS#16333-2018072719352187v1).

2.2. Biochemistry

The concentrations of aspartate and alanine aminotransferases, alkaline phosphatase (ALP) total bilirubin, calcium and phosphate in plasma, were measured on an Olympus AU400 Analyzer. Bile acid concentrations in plasma were determined using the Bile Acid Kit Ecoline S+ (DiaSys Diagnostic Systems GmbH, Holzheim, Germany) on a Hitachi917 analyzer. Hydroxyproline content in liver tissue was measured in lobe 3, using a colorimetric kit from Sigma-Aldrich (Saint-Louis, MO, USA), as previously described [18].

2.3. Histology and (immuno)histochemistry

Formalin (4%)-fixed, paraffin-embedded, mouse and human liver tissue samples were cut into 4-μm-thick sections. Mouse liver tissue sections were stained with hematoxylin and eosin or Sirius red, or were immunostained for cytokeratin 19 (CK19) or F4/80, using an anti-CK19 antibody (TROMA III, Developmental Studies Hybridoma Bank, Iowa University, IA, USA), and an anti-F4/80 antibody (SP115, Abcam, Cambridge, UK), respectively, as described [19, 20]. Stained sections were scanned on a virtual slide

scanner (Hamamatsu, Tokyo, Japan) 2.0 HT, using a 3-charge-coupled device, time-delay integration camera with a resolution of 1.84 µm/pixel (x20 objective) and 0.92 µm/pixel (x40 objective). Morphometric analyses were performed blinded, using ImageJ analysis software (National Institutes of Health, Bethesda, MD, USA). Paraffin-embedded human liver samples stored in the Pathological Department of Saint-Antoine Hospital were provided by this Department. Normal liver sample was from a patient who underwent liver surgery for tumor and pathological liver from a patient with PSC who underwent liver surgery for gallbladder carcinoma. Human liver tissue sections were immunolabeled for PDIA3. First, they were incubated in sodium citrate pH 6, for 20 min at 95°C, to unmask epitopes, and then with 3% bovine serum albumin, to block unspecific binding. Thereafter, sections were incubated with PDIA3 antibody (CL2444, Sigma-Aldrich) diluted 1/100 in Envision flex diluent (Agilent Technologies, Santa Clara, CA, USA), overnight at 4°C. Sections were then incubated with a secondary anti-mouse antibody coupled to Alexa fluor 488 (Invitrogen/Thermo Fisher Scientific, Walthman, MA, USA) diluted 1/200 in 3% bovine serum albumin, at room temperature for one hour. Nuclear staining was performed, using DRAQ5 (Abcam) at 1/1000, for 5 min at room temperature. Tissue sections were examined with a SP2 confocal microscope (Leica, Bannockburn, IL, USA).

2.4. *In vitro* studies

The human biliary epithelial cells Mz-ChA-1 and EGI-1 were obtained from Dr. A. Knuth (Zurich University, Switzerland) and from the German Collection of Microorganisms and Cell Cultures (DSMZ, Braunschweig, Germany), respectively. Although derived from tumor cells, these cell lines can be phenotypically similar to primary biliary epithelial cells [21], and have been validated as surrogate models of cholangiocytes in different settings, including cholestatic liver injury [15, 16, 22-25]. Both Mz-ChA-1 and EGI-1

cells were cultured in DMEM supplemented with 1 g/L glucose, 10 mmol/L HEPES, 10% fetal bovine serum, 100 IU/mL penicillin, 100 µg/mL streptomycin, 0.25 µg/mL amphotericin B (Thermo Fisher Scientific). For transient transfection experiments, Mz-ChA-1 and EGI-1 cells were seeded into 6-well plates (250,000 and 140,000 cells/well, respectively). Cells were transfected with ON-TARGETplus human VDR or PDIA3 siRNA SMARTpools, or siGENOME Non-Targeting siRNA (Horizon Discovery LTD, Cambridge, UK) using DarmaFECT 4 (Horizon Discovery LTD). Seventy-two hours after transfection, cells were incubated with serum-free medium for 12 hours and then treated with tumor necrosis factor (TNF) α (10 ng/mL; Sigma-Aldrich), as previously described [25, 26], combined with calcipotriol (100 nmol/L) [27] or vehicle (DMSO) for 24 hours. Cell lines were routinely screened for the presence of mycoplasma and authenticated for polymorphic markers to prevent cross-contamination.

2.5. Reverse transcription quantitative PCR (RT-qPCR)

Total RNA was extracted using RNeasy columns (Qiagen, Courtaboeuf, France). Complementary DNA was synthesized from total RNA (l µg), using the SuperScript II Reverse Transcriptase (Thermo Fisher Scientific), and qPCR was performed using the Sybr Green Master Mix, on a Light-Cycler 96 (Roche Diagnostics, Basel, Switzerland). Primer sequences are provided in Supporting Table S1. The mRNA levels of target genes were normalized for those of hypoxanthine phosphoribosyltransferase 1 (*Hprt1*) in mouse or glyceraldehyde 3-phosphate dehydrogenase (*GAPDH*) in human, and expressed as relative levels ($2^{-\Delta\Delta Ct}$).

2.6. Immunoblot

Proteins were extracted from liver or colon tissue, separated by 10% SDS-PAGE and transferred to nitrocellulose membranes. Membranes were incubated with primary antibodies raised against PDIA3 (1/2000; ab10287 Abcam), VDR (1/200; sc-13133 Santa

Cruz, Dallas, TX, USA), GAPDH (1/5000; sc-32233 Santa Cruz) or β-Actin (1/2000, A5441 Sigma-Aldrich), overnight at 4°C, and then with secondary, horseradish peroxidase-conjugated antibodies raised against mouse or rabbit IgG (1/2000; Cell Signaling-Ozyme, Saint-Quentin en Yveline, France), for 1 hour at room temperature. Bound antibodies were revealed by enhanced chemiluminescence (Thermo Fischer Scientific). Blots were visualized using ChemiDoc^{TM} Touch Imaging System (BioRad, Hercules, CA, USA) and densitometric analysis was performed using Image Lab^{TM} Software (BioRad).

2.7. Statistics

Data are expressed as mean ± standard deviation, SD. Statistical analyses were performed using GraphPad Prism software version 5.0 (GraphPad Software San Diego, CA, USA). For comparisons between two groups, Mann-Whitney nonparametric *U* test and Student's *t* test were used. Differences between more than two groups were assed using the nonparametric Kruskall-Wallis test followed by Dunn's multiple comparison or one-way ANOVA with Bonferroni post-hoc test. Log-rank test was used to compare Kaplan–Meier survival curves. A *P* value of less than 0.05 was considered significant. Each figure legend states number of experiments performed (*n*), and the statistical test applied.

3. RESULTS

3.1. VDR ablation causes a reduction of lifespan and an increase in the severity of liver injury in *Abcb4* knockout mice

Double knockout ($Vdr^{-/-};Abcb4^{-/-}$) mice were generated and monitored in comparison with simple knockout ($Vdr^{+/+};Abcb4^{-/-}$) littermates, for up to 12 months. $Vdr^{-/-};Abcb4^{-/-}$ mice were viable and showed no overt phenotypic difference with $Vdr^{+/+};Abcb4^{-/-}$ littermates at birth. During follow-up, they showed moderate hypocalcemia compared to $Vdr^{+/+};Abcb4^{-/-}$, whereas the plasma concentrations of phosphate, although transiently lower than in the $Vdr^{+/+};Abcb4^{-/-}$, remained above normal levels (Supplementary Figure S1 C-D). Noticeably, lifespan was significantly reduced in $Vdr^{-/-};Abcb4^{-/-}$ mice as compared to $Vdr^{+/+};Abcb4^{-/-}$ mice, and did not exceed 11 months in these animals (Figure 1A).

To evaluate the impact of *Vdr* invalidation on liver phenotype in $Abcb4^{-/-}$ mice, we performed comparative analyses of liver disease features in $Vdr^{-/-};Abcb4^{-/-}$ and $Vdr^{+/+};Abcb4^{-/-}$ mice at the age of 2 weeks, 4 weeks, 8 weeks and 6 months. Macroscopic examination showed that, compared to simple knockout mice, $Vdr^{-/-};Abcb4^{-/-}$ mice developed more severe hepatomegaly and splenomegaly (Figure 1B). Histological analysis was performed using an adaptation (described in Supplementary Materials and Methods) of Nakamuna scoring [28]. According to this analysis, cholangitis and fibrosis appeared to be more pronounced in $Vdr^{-/-};Abcb4^{-/-}$ mice than in age-matched $Vdr^{+/+};Abcb4^{-/-}$ littermates from 8 weeks on (Figure 1C & Supplementary Table S2).

$Vdr^{-/-};Abcb4^{-/-}$ mice also displayed a rise in the plasma levels of alanine aminotransferase (ALT) (not shown) and aspartate aminotransferase (AST), which from 4 weeks on, were 1.5 to 2.5 higher than those observed in $Vdr^{+/+};Abcb4^{-/-}$ mice (Figure 1D). The plasma levels of ALP also rose to a greater extent in $Vdr^{-/-};Abcb4^{-/-}$ mice than in $Vdr^{+/+};Abcb4^{-/-}$ mice from 4 weeks on, as did those of total bilirubin and bile acids from 8 weeks on (Figure 1D). Taken together these results indicated that $Vdr^{-/-};Abcb4^{-/-}$ mice developed more severe cholestatic liver injury than $Vdr^{+/+};Abcb4^{-/-}$ mice.

3.2. VDR ablation causes an aggravation of cholangiopathy features in *Abcb4* knockout mice

Ductular reaction, which is characterized by a proliferative response of cholangiocytes to injury, is a hallmark of cholangiopathies. We performed CK19 immunostaining on liver tissue sections to assess ductular reaction in the simple and double knockout mice. As previously reported in the *Abcb4* simple knockout mice [29], ductular reaction reached its maximal point both in $Vdr^{+/+};Abcb4^{-/-}$ and $Vdr^{-/-};Abcb4^{-/-}$ mice at the age of 8 weeks, and became less prominent from this point on (Figure 2A). Both at 8 weeks and 6 months, the ductular reaction was significantly more pronounced in $Vdr^{-/-};Abcb4^{-/-}$ mice than in $Vdr^{+/+};Abcb4^{-/-}$ mice (Figure 2A). Thus reactive cholangiocytes were more abundant in $Vdr^{-/-};Abcb4^{-/-}$ mice than in $Vdr^{+/+};Abcb4^{-/-}$ mice.

Reactive cholangiocytes contribute to liver inflammation in cholangiopathies by releasing pro-inflammatory mediators. Therefore, we next assessed the expression of pro-inflammatory factors that are typically produced by reactive cholangiocytes in cholangiopathies in both groups of mice. At the peak time of ductular reaction, *i.e.*, 8

weeks, pro-inflammatory factors including $Tnf\alpha$, vascular cell adhesion molecule 1 (*Vcam1*), C-C motif chemokine ligand (*Ccl*)2, *Ccl20*, *S100a8*, *S100a9* and matrix metalloproteinase 9 (*Mmp9*) were overexpressed in the liver of both $Vdr^{+/+}$;$Abcb4^{-/-}$ and $Vdr^{-/-}$;$Abcb4^{-/-}$ mice, as shown relative to wildtype mice. Importantly, all these genes were expressed at higher levels in $Vdr^{-/-}$;$Abcb4^{-/-}$ mice than in $Vdr^{+/+}$;$Abcb4^{-/-}$ mice (Figure 2B). The overexpression of *Ccl2* and *Ccl20*, which play an essential role in the recruitment of circulating monocytes to injured tissues, was accompanied by an overexpression of their receptors, *i.e.*, CC chemokine receptor *(Ccr)2* and *Ccr6*, respectively (Supplementary Figure S2). Consistent with these results, macrophages were more abundant in the liver of $Vdr^{-/-}$;$Abcb4^{-/-}$ mice than in $Vdr^{+/+}$;$Abcb4^{-/-}$ mice, as ascertained by F4/80 immunostaining (Figure 2C). Altogether these results attested an exacerbation of the immune response in the liver of $Abcb4^{-/-}$ mice in the absence of VDR.

Proinflammatory chemokines and cytokines overproduced in the liver are expected to stimulate liver myofibroblasts and promote liver fibrosis. The quantification of hepatic hydroxyproline content indicated that more collagen accumulated in the liver of $Vdr^{-/-}$;$Abcb4^{-/-}$ mice compared to single knockout mice (Figure 2D, right lower panel). In line with this observation, Sirius red staining showed more extensive liver fibrosis in $Vdr^{-/-}$;$Abcb4^{-/-}$ mice than in $Vdr^{+/+}$;$Abcb4^{-/-}$ mice (Figure 2D, upper, and left lower panels). In agreement with a previous report [30], we observed a stabilization of the liver phenotype in the $Abcb4^{-/-}$ mice (on FVB/N background) with no further aggravation after 8 weeks, and this was true irrespective of the VDR status.

Collectively, these findings indicate that in the absence of VDR, ductular reaction, pro-inflammatory signals and collagen deposition were amplified in the liver of $Abcb4^{-/-}$ mice, highlighting a protective action of VDR in the setting of chronic cholangiopathy.

3.3. Calcipotriol treatment reverses the aggravation of cholangiopathy features in $Vdr^{-/-};Abcb4^{-/-}$ mice

To gain further insights into the protection that vitamin D signaling might confer in the setting of cholangiopathies, we administered a 4-week treatment with calcipotriol, a synthetic vitamin D analog, both in $Vdr^{+/+};Abcb4^{-/-}$ and $Vdr^{-/-};Abcb4^{-/-}$ mice. At the end of treatment, no significant change in blood tests of cholestatic liver injury was observed either in $Vdr^{+/+};Abcb4^{-/-}$ or $Vdr^{-/-};Abcb4^{-/-}$ mice. However, the ductular reaction assessed by CK19 immunostaining was significantly reduced following calcipotriol treatment in $Vdr^{-/-};Abcb4^{-/-}$ mice, whereas it remained unchanged in the $Vdr^{+/+};Abcb4^{-/-}$ mice (Figure 3B). Calcipotriol treatment also elicited a significant decrease in the expression of $Tnf\alpha$, $Ccl2$, $Ccl20$, $S100a8$, $S100a9$ and $Mmp9$ in the liver of $Vdr^{-/-};Abcb4^{-/-}$ mice while no effect on the expression of these factors was found in the liver of $Vdr^{+/+};Abcb4^{-/-}$ mice (Figure 3C). Accordingly, the inflammatory infiltrate assessed by F4/80 immunostaining was reduced in calcipotriol-treated $Vdr^{-/-};Abcb4^{-/-}$ mice compared to the untreated mice (Figure 3D), and fibrosis less severe as shown by a significant difference in hydroxyproline content (Figure 3E). By contrast, calcipotriol treatment had no such effects in $Vdr^{+/+};Abcb4^{-/-}$ mice (Figure 3D). Overall, while calcipotriol treatment did not stop the progression of liver disease in $Vdr^{+/+};Abcb4^{-/-}$ mice, it improved liver

status and reversed the aggravation of cholangiopathy features in $Vdr^{-/-};Abcb4^{-/-}$ mice. This indicated that the vitamin D analog activated a VDR-independent pathway that attenuated the severity of cholangiopathy in the double knockout mice.

3.4. PDIA3 is overexpressed in the liver and cholangiocytes of $Vdr^{-/-};Abcb4^{-/-}$ mice

PDIA3, the membrane receptor of vitamin D, mediates anti-inflammatory actions by mechanisms such as the ectodomain shedding of TNF receptor 1 [31, 32]. We hypothesized that the VDR-independent effects of calcipotriol observed in $Vdr^{-/-};Abcb4^{-/-}$ mice, could be mediated by PDIA3. Consistent with this hypothesis, we found that hepatic *Pdia3* mRNA and protein expression was significantly increased in $Vdr^{-/-};Abcb4^{-/-}$ mice compared to wildtype (FVB/N) and $Vdr^{+/+};Abcb4^{-/-}$ mice (Figure 4, A and B). Looking into pools of individual liver cell types that were isolated from wildtype and simple *Abcb4* knockout mice, we found that they all expressed *Pdia3*, but that *Pdia3* expression increased distinctively in cholangiocytes from *Abcb4* knockout mice compared to wildtype, whereas little change occurred in the other cell types (Figure 4C). We also examined *Pdia3* expression specifically in cholangiocytes from $Vdr^{-/-};Abcb4^{-/-}$ mice, and found an even higher expression than in the simple knockout and wildtype mice (Figure 4D). Because cholangiocytes i) are more numerous and ii) express more *Pdia3* in the liver of $Vdr^{-/-};Abcb4^{-/-}$ mice than in the wildtype and simple *Abcb4* knockout mice, we inferred that they accounted at least partly for *Pdia3* overexpression in the liver of the double knockout. We could also show that in the liver tissue from a patient with PSC, PDIA3 was immunodetected in cholangiocytes of both small and large bile ducts and localized at their plasma membrane where it could mediate vitamin D effects (Figure 4E). Moreover, the intensity of labeling in cholangiocytes appeared to be higher in PSC than

in normal liver (Figure 4E). Collectively, our results indicated that cholangiocytes are a major site of PDIA3 expression in cholangiopathy.

3.5. PDIA3 mediates VDR-independent anti-inflammatory effects of calcipotriol in cholangiocytes

To examine whether PDIA3 in cholangiocytes could contribute to VDR-independent effects of calcipotriol in $Vdr^{-/-};Abcb4^{-/-}$ mice, we invalidated VDR and PDIA3 in human cholangiocytes. Two human biliary epithelial cell lines, Mz-ChA-1 and EGI-1, commonly studied as surrogate models of non-tumoral human cholangiocytes [15, 16, 21-25], were transfected with *VDR* ± *PDIA3* siRNA (Supplementary Figure S3, A and B). *VDR* knockdown caused a significant increase in the expression of pro-inflammatory factors that were found to be overexpressed in the liver of $Vdr^{-/-};Abcb4^{-/-}$ mice, including *CCL2*, *CCL20*, *S100A9* and *MMP9* in MzChA-1 cells (Figure 5A), and *CCL20*, *S100A9* and *MMP9* in EGI-1 (Supplementary Figure S4A). Similar variations of these factors were observed in cholangiocytes isolated from the double compared to simple knockout mice, even though only the difference in *Ccl20* expression reached statistical significance (Supplementary Figure S5). *VDR* knockdown also caused a significant increase in PDIA3 in human biliary epithelial cell lines (Supplementary Figure S3, A and B). Next, we tested the effect of calcipotriol in the context of cholangiocyte inflammatory response to TNFα [25, 26]. TNFα induced a marked increase in the expression of *CCL2*, *CCL20, S100A9* and *MMP9* in Mz-ChA-1 cells (Figure 5B). Calcipotriol significantly reduced the rise triggered by TNFα in the expression of *CCL2*, *CCL20* and *MMP9* in these cells (Figure 5B). The inhibitory effect of calcipotriol was also observed in the cells silenced for VDR, whereas no such effect occurred in the cells silenced for both VDR and PDIA3 (Figure 5B). EGI-1 cells also displayed an overexpression of *CCL20, S100A9* and *MMP9*, when silenced for VDR (Supplementary Figure S4A). Although they were poorly

responsive to TNFα in basal conditions, the overexpression of *S100A9* and *MMP9* induced by TNFα was reduced by calcipotriol in cells lacking VDR, but not in those lacking both VDR and PDIA3 (Supplementary Figure S4B). Taken together, these results indicated that in the absence of VDR, PDIA3 mediated anti-inflammatory effects of calcipotriol in the liver, which may have contributed to the protective effects of calcipotriol observed in *Vdr*^{-/-};*Abcb4*^{-/-} mice.

3.6. Long-term vitamin D supplementation alleviates the severity of cholangiopathy phenotype in *Vdr*^{-/-};*Abcb4*^{-/-} mice

To further confirm that vitamin D can elicit VDR-independent protective mechanisms in cholangiopathy, we tested long-term natural vitamin D supplementation in the *Abcb4* knockout mice. *Vdr*^{+/+};*Abcb4*^{-/-} and *Vdr*^{-/-};*Abcb4*^{-/-} mice were fed a vitamin D-enriched diet from weaning until the age of 6 months. Akin to short-term pharmacological treatment with calcipotriol, long-term vitamin D supplementation improved cholangiopathy features in *Vdr*-invalidated *Abcb4* knockout mice. Cholestasis, ductular reaction and liver fibrosis were all significantly less intense in the double knockout mice who received vitamin D supplementation for 6 months compared to those who were fed a regular chow diet (Figure 6, A-C). By contrast, no improvement resulted from vitamin D supplementation in the *Vdr*^{+/+};*Abcb4*^{-/-} mice even though we observed a significant reduction of ALP levels which might reflect an improvement by vitamin D supplementation of the hepatic osteodystrophy that occurs in *Abcb4*^{-/-} mice [33].

Consistent with these results, long-term vitamin D supplementation improved survival rates only in *Vdr*^{-/-};*Abcb4*^{-/-} mice (Figure 6D). These results confirmed the existence of

an alternative vitamin D signaling pathway independent of VDR, which promotes protective mechanisms in cholangiopathy.

4. DISCUSSION

In this study, we demonstrate the protective functions of VDR in a mouse model of chronic cholangiopathy. Cholestasis, hepatic inflammation and fibrosis were exacerbated by the loss of VDR in *Abcb4* knockout mice. Yet, the activation of VDR by vitamin D or calcipotriol treatments failed to ameliorate cholangiopathy in *Abcb4* knockout mice. Instead, vitamin D and calcipotriol treatments improved liver injury in the *Abcb4* knockout mice that lacked VDR, implying the existence of VDR-independent protective effects of vitamin D and analog in this model. Our data provide evidence to indicate that VDR-independent actions of vitamin D in this context may be mediated by PDIA3. Biochemical markers of liver injury and inflammation were increased in *Abcb4* knockout mice in the absence of VDR. *Vdr* knockout mice on a C57BL/6J background spontaneously develop hepatic inflammation and fibrosis at the age of 6 months [27, 34]. These observation have been attributed to anti-inflammatory and anti-fibrotic effects of VDR in liver macrophages [34] and hepatic stellate cells [27], respectively. Without excluding that these effects contributed to the development of a more severe liver phenotype in $Vdr^{-/-}$;$Abcb4^{-/-}$ mice compared to $Vdr^{+/+}$;$Abcb4^{-/-}$, we herein specifically addressed the contribution of *Vdr* loss in cholangiocytes. The first reason is that VDR expression in the liver, is most prominent in cholangiocytes than in any other liver cell type, both in humans [15] and in mice, especially in the context of chronic cholangiopathy, as shown in *Abcb4* knockout mice [13]. The second reason is that cholangiocytes are proliferative and produce pro-inflammatory factors in cholangiopathies, whereby they promote fibrosis and disease progression in these disorders [1]. We found that cholangiocytes lacking VDR overexpressed pro-inflammatory factors both *in vivo* and *in vitro*. Moreover, cholangiocytes lacking VDR were more proliferative *in vivo* (Figure 2A), suggesting that cholangiocytes played a

significant role in the aggravation of cholangiopathy caused by VDR loss. While VDR has been shown to promote epithelial barrier integrity [16, 35], we could not detect more bile duct disruption in $Vdr^{-/-}$ mice than in $Vdr^{+/+}$ mice in the chronic model of $Abcb4$ invalidation (Supplementary Figure S6). Neither did we detect a significant increase in the permeability or histology of the intestine of $Vdr^{-/-};Abcb4^{-/-}$ compared to $Vdr^{+/+};Abcb4^{-/-}$ mice (Supplementary Figure S7).

Activation of VDR by vitamin D analogs has been considered as a therapeutic option in chronic liver diseases. Supporting this strategy, hypocalcemic vitamin D analogs approved for use in patients (*i.e.* calcipotriol, for topical treatments; alfacalcidol and paricalcitol for systemic treatments), have demonstrated antifibrotic properties both in hepatic stellate cells *in vitro* [27, 36], and in mouse models of CCl_4- and- thioacetamide-induced liver fibrosis *in vivo* [27, 36, 37]. Calcipotriol used as a prophylactic treatment has also been shown to prevent biliary fibrosis induced by bile duct ligation or 3,5-diethoxycarbonyl-1,4-dihydrocollidine (DDC) in mice [38]. However, when used as a curative treatment, calcipotriol herein failed to improve liver fibrosis in $Abcb4$ knockout mice. Liver fibrosis in $Abcb4$ knockout mice was left unchanged by treatments with active vitamin D (calcitriol), or a high-dose vitamin D diet, as shown here and in a previous study [6, 39]. Yet, $Abcb4$ knockout mice on low vitamin D diet display aggravated liver fibrosis, which in this particular case, can be ameliorated by a vitamin D-sufficient diet [6]. Importantly, in such case, a high vitamin D supplementation adds no benefit over a normal intake [6]. Taken together, these data indicate that normal levels of vitamin D are sufficient to ensure VDR-dependent protective mechanisms in cholangiopathies. They suggest that in a setting of effective VDR signaling, increasing VDR ligands does not provide further therapeutic benefit.

Remarkably, we found that both high-dose vitamin D supplementation and a vitamin D analog were beneficial in *Abcb4* knockout mice lacking VDR, highlighting VDR-independent protective effects of vitamin D. We postulated that VDR-independent protective effects of vitamin D and analogs in the liver, could be mediated by PDIA3, the membrane receptor of vitamin D [11]. Consistent with this assumption, we could show that PDIA3 was expressed at high levels in cholangiocytes of *Abcb4* knockout mice. Furthermore, pro-inflammatory response was suppressed by calcipotriol acting *via* PDIA3 in cholangiocytes, as demonstrated *in vitro*. In keeping with this result, PDIA3 was previously shown to mediate nongenomic actions of vitamin D by shedding the ectodomain of TNF receptor 1, thus decreasing responsiveness to TNFα [31]. Noteworthily, this mechanism is activated by Vitamin D3 and derivatives [32], to which calipotriol belongs. The binding potency of vitamin D for PDIA3 is lower than for VDR [40], suggesting that vitamin D or calcipotriol preferentially bind to VDR in cells that express both receptors. Therefore, we suggest that PDIA3 mediates anti-inflammatory effects of vitamin D particularly in the context of defective VDR signaling, when the ligand bioavailability is increased and PDIA3 overexpressed, as shown here and in a previous study [41]. Nevertheless, specific ligands of this receptor are currently lacking and need to be developed to further explore the role of PDIA3 in the inflammatory response of cholangiocytes.

The clinical relevance of our findings is supported by previous studies showing that in subjects with liver disease, VDR gene variants can lead to low VDR expression in the liver, which is associated with a higher severity of inflammation and fibrosis [42, 43]. Therefore, while a treatment aimed to maintain normal levels of vitamin D may be sufficient in a large number of patients with cholangiopathies, a subset of patients could benefit from Vitamin D treatments *via* PDIA3. Further studies are needed to determine

the impact of VDR polymorphisms on disease progression (prognosis, severity or risk of cancer development) in patients with cholangiopathies. This may help to identify subgroup of patients that would benefit from treatments with supra-physiological doses of vitamin D. Furthermore, additional strategies aimed to boost PDIA3 anti-inflammatory effects with PDIA3-specific ligands may be of clinical interest regardless of VDR expression status. The present study provides rationale to explore this strategy in the future.

In conclusion, the present findings provide new mechanistic insights into the involvement of vitamin D signaling in cholangiocytes and cholangiopathies. They indicate that the VDR status of patients with cholangiopathies may be as important as circulating vitamin D levels in these diseases. Moreover, our data provide evidence for PDIA3 anti-inflammatory effects in cholangiocytes, suggesting a potential interest as a therapeutic target in cholangiopathies.

REFERENCES

[1] J.M. Banales, R.C. Huebert, T. Karlsen, M. Strazzabosco, N.F. LaRusso, G.J. Gores, Cholangiocyte pathobiology, Nat Rev Gastroenterol Hepatol, 16 (2019) 269-281.

[2] S. Petta, C. Camma, C. Scazzone, C. Tripodo, V. Di Marco, A. Bono, D. Cabibi, G. Licata, R. Porcasi, G. Marchesini, A. Craxi, Low vitamin D serum level is related to severe fibrosis and low responsiveness to interferon-based therapy in genotype 1 chronic hepatitis C, Hepatology, 51 (2010) 1158-1167.

[3] E. Trepo, R. Ouziel, P. Pradat, Y. Momozawa, E. Quertinmont, C. Gervy, T. Gustot, D. Degre, V. Vercruysse, P. Deltenre, L. Verset, B. Gulbis, D. Franchimont, J. Deviere, A. Lemmers, C. Moreno, Marked 25-hydroxyvitamin D deficiency is associated with poor prognosis in patients with alcoholic liver disease, Journal of hepatology, 59 (2013) 344-350.

[4] T. Arai, M. Atsukawa, A. Tsubota, M. Koeda, Y. Yoshida, T. Okubo, A. Nakagawa, N. Itokawa, C. Kondo, K. Nakatsuka, T. Masu, K. Kato, N. Shimada, T. Hatori, N. Emoto, M. Kage, K. Iwakiri, Association of vitamin D levels and vitamin D-related gene polymorphisms with liver fibrosis in patients with biopsy-proven nonalcoholic fatty liver disease, Dig Liver Dis, 51 (2019) 1036-1042.

[5] A.J. Czaja, A.J. Montano-Loza, Evolving Role of Vitamin D in Immune-Mediated Disease and Its Implications in Autoimmune Hepatitis, Dig Dis Sci, 64 (2019) 324-344.

[6] K. Hochrath, C.S. Stokes, J. Geisel, M.J. Pollheimer, P. Fickert, S. Dooley, F. Lammert, Vitamin D modulates biliary fibrosis in ABCB4-deficient mice, Hepatol Int, 8 (2014) 443-452.

[7] T.H. Mauad, C.M. van Nieuwkerk, K.P. Dingemans, J.J. Smit, A.H. Schinkel, R.G. Notenboom, M.A. van den Bergh Weerman, R.P. Verkruisen, A.K. Groen, R.P. Oude Elferink, et al., Mice with homozygous disruption of the mdr2 P-glycoprotein gene. A novel animal model for studies of nonsuppurative inflammatory cholangitis and hepatocarcinogenesis, The American journal of pathology, 145 (1994) 1237-1245.

[8] P. Fickert, A. Fuchsbichler, M. Wagner, G. Zollner, A. Kaser, H. Tilg, R. Krause, F. Lammert, C. Langner, K. Zatloukal, H.U. Marschall, H. Denk, M. Trauner, Regurgitation of bile acids from leaky bile ducts causes sclerosing cholangitis in Mdr2 (Abcb4) knockout mice, Gastroenterology, 127 (2004) 261-274.

[9] Y. Popov, E. Patsenker, P. Fickert, M. Trauner, D. Schuppan, Mdr2 (Abcb4)-/- mice spontaneously develop severe biliary fibrosis via massive dysregulation of pro- and antifibrogenic genes, Journal of hepatology, 43 (2005) 1045-1054.

[10] P. Fickert, M.J. Pollheimer, U. Beuers, C. Lackner, G. Hirschfield, C. Housset, V. Keitel, C. Schramm, H.U. Marschall, T.H. Karlsen, E. Melum, A. Kaser, B. Eksteen, M. Strazzabosco, M. Manns, M. Trauner, P.S.C.S.G. International, Characterization of animal models for primary sclerosing cholangitis (PSC), Journal of hepatology, 60 (2014) 1290-1303.

[11] A. Hettinghouse, R. Liu, C.J. Liu, Multifunctional molecule ERp57: From cancer to neurodegenerative diseases, Pharmacol Ther, 181 (2018) 34-48.

[12] M. Gascon-Barre, C. Demers, A. Mirshahi, S. Neron, S. Zalzal, A. Nanci, The normal liver harbors the vitamin D nuclear receptor in nonparenchymal and biliary epithelial cells, Hepatology, 37 (2003) 1034-1042.

[13] E. Gonzalez-Sanchez, D. Firrincieli, C. Housset, N. Chignard, Expression patterns of nuclear receptors in parenchymal and non-parenchymal mouse liver cells and their modulation in cholestasis, Biochim Biophys Acta Mol Basis Dis, 1863 (2017) 1699-1708.

[14] A. Vogel, C.P. Strassburg, M.P. Manns, Genetic association of vitamin D receptor polymorphisms with primary biliary cirrhosis and autoimmune hepatitis, Hepatology, 35 (2002) 126-131.

[15] E. D'Aldebert, M.J. Biyeyeme Bi Mve, M. Mergey, D. Wendum, D. Firrincieli, A. Coilly, L. Fouassier, C. Corpechot, R. Poupon, C. Housset, N. Chignard, Bile salts control the antimicrobial peptide cathelicidin through nuclear receptors in the human biliary epithelium, Gastroenterology, 136 (2009) 1435-1443.

[16] D. Firrincieli, S. Zuniga, C. Rey, D. Wendum, E. Lasnier, D. Rainteau, T. Braescu, T. Falguieres, M. Boissan, A. Cadoret, C. Housset, N. Chignard, Vitamin D nuclear receptor deficiency promotes cholestatic liver injury by disruption of biliary epithelial cell junctions in mice, Hepatology, 58 (2013) 1401-1412.

[17] M.H. Sherman, R.T. Yu, D.D. Engle, N. Ding, A.R. Atkins, H. Tiriac, E.A. Collisson, F. Connor, T. Van Dyke, S. Kozlov, P. Martin, T.W. Tseng, D.W. Dawson, T.R. Donahue, A. Masamune, T. Shimosegawa, M.V. Apte, J.S. Wilson, B. Ng, S.L. Lau, J.E. Gunton, G.M. Wahl, T. Hunter, J.A. Drebin, P.J. O'Dwyer, C. Liddle, D.A. Tuveson, M. Downes, R.M. Evans, Vitamin D receptor-mediated stromal reprogramming suppresses pancreatitis and enhances pancreatic cancer therapy, Cell, 159 (2014) 80-93.

[18] I.S. Jamall, V.N. Finelli, S.S. Que Hee, A simple method to determine nanogram levels of 4-hydroxyproline in biological tissues, Anal Biochem, 112 (1981) 70-75.

[19] D. Debray, H. El Mourabit, F. Merabtene, L. Brot, D. Ulveling, Y. Chretien, D. Rainteau, I. Moszer, D. Wendum, H. Sokol, C. Housset, Diet-Induced Dysbiosis and Genetic Background Synergize With Cystic Fibrosis Transmembrane Conductance Regulator Deficiency to Promote Cholangiopathy in Mice, Hepatol Commun, 2 (2018) 1533-1549.

[20] A. Majdi, L. Aoudjehane, V. Ratziu, T. Islam, M.B. Afonso, F. Conti, T. Mestiri, M. Lagouge, F. Foufelle, F. Ballenghien, T. Ledent, M. Moldes, A. Cadoret, L. Fouassier, J.L. Delaunay, T. Ait-Slimane, G. Courtois, B. Feve, O. Scatton, C. Prip-Buus, C.M.P. Rodrigues, C. Housset, J. Gautheron, Inhibition of receptor-interacting protein kinase 1 improves experimental non-alcoholic fatty liver disease, Journal of hepatology, 72 (2020) 627-635.

[21] S. Basavappa, J. Middleton, A.W. Mangel, J.M. McGill, J.A. Cohn, J.G. Fitz, Cl-and K+ transport in human biliary cell lines, Gastroenterology, 104 (1993) 1796-1805.

[22] W. Stremmel, S. Staffer, R. Weiskirchen, Phosphatidylcholine Passes by Paracellular Transport to the Apical Side of the Polarized Biliary Tumor Cell Line Mz-ChA-1, International journal of molecular sciences, 20 (2019).

[23] S. Hohenester, L.M. Wenniger, C.C. Paulusma, S.J. van Vliet, D.M. Jefferson, R.P. Elferink, U. Beuers, A biliary HCO3- umbrella constitutes a protective mechanism against bile acid-induced injury in human cholangiocytes, Hepatology, 55 (2012) 173-183.

[24] L. Fouassier, P. Rosenberg, M. Mergey, B. Saubamea, A. Claperon, N. Kinnman, N. Chignard, G. Jacobsson-Ekman, B. Strandvik, C. Rey, V. Barbu, R. Hultcrantz, C. Housset, Ezrin-radixin-moesin-binding phosphoprotein (EBP50), an estrogen-inducible scaffold protein, contributes to biliary epithelial cell proliferation, The American journal of pathology, 174 (2009) 869-880.

[25] A. Baghdasaryan, T. Claudel, A. Kosters, J. Gumhold, D. Silbert, A. Thuringer, K. Leski, P. Fickert, S.J. Karpen, M. Trauner, Curcumin improves sclerosing cholangitis in Mdr2-/- mice by inhibition of cholangiocyte inflammatory response and portal myofibroblast proliferation, Gut, 59 (2010) 521-530.

[26] C.J. Soroka, D.N. Assis, L.S. Alrabadi, S. Roberts, L. Cusack, A.B. Jaffe, J.L. Boyer, Bile-Derived Organoids From Patients With Primary Sclerosing Cholangitis Recapitulate Their Inflammatory Immune Profile, Hepatology, 70 (2019) 871-882.

[27] N. Ding, R.T. Yu, N. Subramaniam, M.H. Sherman, C. Wilson, R. Rao, M. Leblanc, S. Coulter, M. He, C. Scott, S.L. Lau, A.R. Atkins, G.D. Barish, J.E. Gunton, C. Liddle,

M. Downes, R.M. Evans, A vitamin D receptor/SMAD genomic circuit gates hepatic fibrotic response, Cell, 153 (2013) 601-613.

[28] E.M. de Vries, M. de Krijger, M. Farkkila, J. Arola, P. Schirmacher, D. Gotthardt, B. Goeppert, P.J. Trivedi, G.M. Hirschfield, H. Ytting, B. Vainer, H.R. Buuren, K. Biermann, M.H. Harms, O. Chazouilleres, D. Wendum, A.D. Kemgang, R.W. Chapman, L.M. Wang, K.D. Williamson, A.S. Gouw, V. Paradis, C. Sempoux, U. Beuers, S.G. Hubscher, J. Verheij, C.Y. Ponsioen, Validation of the prognostic value of histologic scoring systems in primary sclerosing cholangitis: An international cohort study, Hepatology, 65 (2017) 907-919.

[29] S.Y. Cai, A. Mennone, C.J. Soroka, J.L. Boyer, Altered expression and function of canalicular transporters during early development of cholestatic liver injury in Abcb4-deficient mice, Am J Physiol Gastrointest Liver Physiol, 306 (2014) G670-676.

[30] N. Ikenaga, S.B. Liu, D.Y. Sverdlov, S. Yoshida, I. Nasser, Q. Ke, P.M. Kang, Y. Popov, A new Mdr2(-/-) mouse model of sclerosing cholangitis with rapid fibrosis progression, early-onset portal hypertension, and liver cancer, The American journal of pathology, 185 (2015) 325-334.

[31] W.S. Yang, H.W. Kim, J.M. Lee, N.J. Han, M.J. Lee, S.K. Park, 1,25-dihydroxyvitamin D3 causes ADAM10-dependent ectodomain shedding of tumor necrosis factor receptor 1 in vascular smooth muscle cells, Mol Pharmacol, 87 (2015) 533-542.

[32] W.S. Yang, H. Yu, J.J. Kim, M.J. Lee, S.K. Park, Vitamin D-induced ectodomain shedding of TNF receptor 1 as a nongenomic action: D3 vs D2 derivatives, J Steroid Biochem Mol Biol, 155 (2016) 18-25.

[33] K. Hochrath, S. Ehnert, C.L. Ackert-Bicknell, Y. Lau, A. Schmid, M. Krawczyk, J.G. Hengstler, J. Dunn, K. Hiththetiya, B. Rathkolb, K. Micklich, W. Hans, H. Fuchs, V. Gailus-Durner, E. Wolf, M.H. de Angelis, S. Dooley, B. Paigen, B. Wildemann, F. Lammert, A.K. Nussler, Modeling hepatic osteodystrophy in Abcb4 deficient mice, Bone, 55 (2013) 501-511.

[34] B. Dong, Y. Zhou, W. Wang, J. Scott, K. Kim, Z. Sun, Q. Guo, Y. Lu, N.M. Gonzales, H. Wu, S.M. Hartig, R.B. York, F. Yang, D.D. Moore, Vitamin D Receptor Activation in Liver Macrophages Ameliorates Hepatic Inflammation, Steatosis, and Insulin Resistance in Mice, Hepatology, 71 (2020) 1559-1574.

[35] J. Kong, Z. Zhang, M.W. Musch, G. Ning, J. Sun, J. Hart, M. Bissonnette, Y.C. Li, Novel role of the vitamin D receptor in maintaining the integrity of the intestinal mucosal barrier, Am J Physiol Gastrointest Liver Physiol, 294 (2008) G208-216.

[36] F.P. Reiter, L. Ye, F. Bosch, R. Wimmer, R. Artmann, A. Ziesch, V. Kanitz, D. Mayr, C.J. Steib, M. Trauner, I. Regel, A.L. Gerbes, J. Mayerle, S. Hohenester, E.N. de Toni, G. Denk, Antifibrotic effects of hypocalcemic vitamin D analogs in murine and human hepatic stellate cells and in the CCl4 mouse model, Laboratory investigation; a journal of technical methods and pathology, 99 (2019) 1906-1917.

[37] E. Wahsh, N. Abu-Elsaad, A. El-Karef, T. Ibrahim, The vitamin D receptor agonist, calcipotriol, modulates fibrogenic pathways mitigating liver fibrosis in-vivo: An experimental study, Eur J Pharmacol, 789 (2016) 362-369.

[38] X. Wang, G. Wang, J. Qu, Z. Yuan, R. Pan, K. Li, Calcipotriol Inhibits NLRP3 Signal Through YAP1 Activation to Alleviate Cholestatic Liver Injury and Fibrosis, Frontiers in pharmacology, 11 (2020) 200.

[39] F.P. Reiter, S. Hohenester, J.M. Nagel, R. Wimmer, R. Artmann, L. Wottke, M.C. Makeschin, D. Mayr, C. Rust, M. Trauner, G.U. Denk, 1,25-(OH)(2)-vitamin D(3) prevents activation of hepatic stellate cells in vitro and ameliorates inflammatory liver

damage but not fibrosis in the Abcb4(-/-) model, Biochem Biophys Res Commun, 459 (2015) 227-233.

[40] C. Tohda, T. Urano, M. Umezaki, I. Nemere, T. Kuboyama, Diosgenin is an exogenous activator of 1,25D(3)-MARRS/Pdia3/ERp57 and improves Alzheimer's disease pathologies in 5XFAD mice, Scientific reports, 2 (2012) 535.

[41] J. Chen, M. Doroudi, J. Cheung, A.L. Grozier, Z. Schwartz, B.D. Boyan, Plasma membrane Pdia3 and VDR interact to elicit rapid responses to 1alpha,25(OH)(2)D(3), Cell Signal, 25 (2013) 2362-2373.

[42] S. Petta, S. Grimaudo, C. Tripodo, D. Cabibi, M. Calvaruso, A. Di Cristina, C. Guarnotta, F.S. Macaluso, M.G. Minissale, G. Marchesini, A. Craxi, The hepatic expression of vitamin D receptor is inversely associated with the severity of liver damage in genotype 1 chronic hepatitis C patients, J Clin Endocrinol Metab, 100 (2015) 193-200.

[43] A. Beilfuss, J.P. Sowa, S. Sydor, M. Beste, L.P. Bechmann, M. Schlattjan, W.K. Syn, I. Wedemeyer, Z. Mathe, C. Jochum, G. Gerken, R.K. Gieseler, A. Canbay, Vitamin D counteracts fibrogenic TGF-beta signalling in human hepatic stellate cells both receptor-dependently and independently, Gut, 64 (2015) 791-799.

FIGURE LEGENDS

Figure 1. VDR ablation has a deleterious impact on the phenotype of *Abcb4* knockout mice.

Vdr$^{-/-}$;*Abcb4*$^{-/-}$ compared to *Vdr*$^{+/+}$;*Abcb4*$^{-/-}$ mice showed (A) a reduction of survival estimated by the Kaplan-Meier method (*n*=15 mice per group) and (B-D) more severe course of liver disease, as indicated by analyses at different time points of (B) liver weight and spleen weight to body weight ratios (*n*=8-14 mice per group); (C) hematoxylin and eosin-stained liver tissue sections (arrowheads point to onion-skin type fibrosis and fibrotic septa) and (D) plasma concentrations of aspartate aminotransferase (AST), alkaline phosphatase (ALP), total bilirubin and bile acids (*n*=5-10 mice per group). Bar graphs represent means ± SD; dashed lines represent the mean values in *n*=6 (8 weeks old) wildtype (WT) mice; *P<0.05; **P<0.01; ***P<0.001; ****P<0.0001 (Log-rank test for A; Mann-Whitney *U* test for B and D). Scale bars = 500 μm.

Figure. 2. VDR ablation aggravates cholangiopathy features in *Abcb4* knockout mice.

Vdr$^{-/-}$;*Abcb4*$^{-/-}$ compared to *Vdr*$^{+/+}$;*Abcb4*$^{-/-}$ mice showed more severe cholangiopathy as indicated by analyses at different time points of (A) ductular reaction assessed by cytokeratin 19 (CK19) immunostaining (*n*=6-7 mice per group), (B-C) hepatic inflammation assessed by (B) RT-qPCR of tumor necrosis factor α (*Tnfα*), vascular cell adhesion molecule 1 (*Vcam1*), C-C motif chemokine ligand (*Ccl*) *2*, *Ccl20*, *S100a8*, *S100a9*, matrix metalloproteinase 9 (*Mmp9*) (*n*=6-9 mice per group), expressed relative to a pool of hepatic mRNA from *n*=8 (8 weeks old) wildtype (WT) mice and (C) F4/80 immunostaining of macrophages (*n*=6-7 mice per group). (D) liver fibrosis assessed by Sirius red staining and hydroxyproline content (*n*=7-8 mice per group). Bar graphs represent means ± SD; dashed lines represent the mean values in *n*=6 (8 weeks old) WT

mice; *$P<0.05$; **$P<0.01$; ***$P<0.001$ (Mann-Whitney U test). Scale bars = 250 μm in A and C, and 500 μm in D.

Figure. 3. Calcipotriol treatment reverses the aggravation of cholangiopathy features elicited by the lack of VDR in *Abcb4* knockout mice.

Vdr$^{+/+}$;*Abcb4*$^{-/-}$ and *Vdr*$^{-/-}$;*Abcb4*$^{-/-}$ mice received intraperitoneal injections of calcipotriol (40 μg/kg) or vehicle, 3 times a week from the age of 4 weeks to 8 weeks, and upon sacrifice at 8 weeks, their liver phenotype was assessed by (A) Plasma concentrations of aspartate aminotransferase (AST), alkaline phosphatase (ALP), total bilirubin and bile acids (*n*=5-8 mice per group). (B) Cytokeratin 19 (CK19) immunostaining (*n*= 7-8 mice per group). (C) RT-qPCR analyses of the pro-inflammatory factors, tumor necrosis factor α (*Tnfα*), vascular cell adhesion molecule 1 (*Vcam1*), C-C motif chemokine ligand *(Ccl) 2*, *Ccl20*, *S100a8*, *S100a9* and matrix metalloproteinase 9 (*Mmp9*), in liver (*n*=7-8 mice per group), expressed relative to a pool of hepatic mRNA from 8 (8 weeks old) wildtype (WT) mice. (D) F4/80 immunostaining of macrophages (*n*=6-7 mice per group). (E) Sirius red staining and hydroxyproline content in liver (*n*=7-8 mice per group). Bar graphs represent means ± SD; dashed lines in A represent mean baseline values at the starting point of calcipotriol treatment in 4 weeks old *Vdr*$^{+/+}$;*Abcb4*$^{-/-}$ and *Vdr*$^{-/-}$;*Abcb4*$^{-/-}$ mice. *$P<0.05$ (Mann-Whitney U test). Scale bars = 250 μm in B and D, and 500 μm in E.

Figure 4. Protein disulfide-isomerase A3 (PDIA3) is overexpressed in the liver and cholangiocytes of *Abcb4* knockout mice lacking VDR.

PDIA3 expression was analyzed in (A-D) 8 weeks old mice (A-B) whole liver from *n*=6-9 per group by RT-qPCR and by immunoblot; (C) individual liver cell populations (*n*=1 mRNA pool from 6-8 mice) by RT-qPCR; In A and C, results are expressed relative to a pool of hepatic mRNA from *n*=8 wildtype (WT) mice); (D) in cholangiocytes (*n*=3 different mRNA pools from 3-4 mice) by RT-qPCR (results are expressed relative to a

pool of cholangiocyte mRNA from n=8 WT mice; numbers within bars represent Ct values); (E) in tissue sections of normal human liver or liver from a patient with PSC; representative images highlight PDIA3 expression at the plasma membrane of cholangiocytes, both in small and large bile ducts (arrows and inset). Bar graphs represent means ± SD; *P<0.05 (Kurskall-Wallis test followed by Dunn's multiple comparison);. Hep, hepatocytes; Chol, cholangiocytes; HSC, hepatic stellate cells; LSEC, liver sinusoidal endothelial cells; KC, Kupffer cells. Scale bars = 10 μm.

Figure 5. The lack of VDR triggers a pro-inflammatory response in biliary epithelial cells that is counteracted by calcipotriol *via* PDIA3.

The expression of the proinflammatory factors, tumor necrosis factor α (TNFα), vascular cell adhesion molecule 1 (*VCAM1*), C-C motif chemokine ligand (CCL) 2, CCL20, S100A8, S100A9 and/or matrix metalloproteinase 9 (MMP9), was measured by RT-qPCR in the human biliary epithelial cells Mz-ChA-1, that were transfected with scramble siRNA, or *VDR* siRNA alone or combined with *PDIA3* siRNA, and 96 hours after transfection, analyzed in (A) basal conditions (n=8-10 independent experiments), or (B) incubated with vehicle or TNFα (10 ng/mL) with or without calcipotriol (100 nmol/L) for 24 hours (n=8 independent experiments). Bar graphs represent means ± SD; *P<0.05; **P<0.01 (paired Student t test for A; one-way ANOVA with Bonferroni post-hoc test for B). ND, not detected.

Figure 6. Long-term vitamin D supplementation reduces the severity of cholangiopathy features in Abcb4 knockout mice lacking VDR.

Vdr$^{+/+}$;*Abcb4*$^{-/-}$ and *Vdr*$^{-/-}$;*Abcb4*$^{-/-}$ mice were fed a regular or vitamin D (VD) supplemented diet after weaning, and upon sacrifice at 6 months, they underwent analyses of liver phenotype. (A) plasma concentrations of aspartate aminotransferase (AST), alkaline phosphatase (ALP), total bilirubin and bile acids (n=6-8 mice per group). (B)

Cytokeratin 19 (CK19) immunostaining (n=6-7 mice per group). (C) Sirius red staining and hydroxyproline content in liver (n= 7 mice per group). (D) Survival curves calculated by the Kaplan-Meier method in *Vdr*$^{+/+}$;*Abcb4*$^{-/-}$ and *Vdr*$^{-/-}$;*Abcb4*$^{-/-}$ mice, fed a regular or vitamin D (VD) supplemented diet (n=15 mice per group). Bar graphs represent means ± SD; *P<0.05; **P<0.01 (Mann-Whitney *U* test for A-C; Log-rank test for D). Scale bars = 250 μm and 500 μm in B and C, respectively.

Cholangiopathy aggravation is caused by VDR ablation and alleviated by VDR-independent vitamin D signaling in ABCB4 knockout mice

Ester Gonzalez-Sanchez [a,b,c,*,1], Haquima El Mourabit [a], Marion Jager [a], Marie Clavel [a,b], Sophie Moog [a,b], Javier Vaquero [a,c,d,1], Tatiana Ledent [a], Axelle Cadoret [a], Jérémie Gautheron [a], Laura Fouassier [a], Dominique Wendum [a,e], Nicolas Chignard [b,#], Chantal Housset [a,f,*,#]

[a]Sorbonne Université, INSERM, Centre de Recherche Saint-Antoine (CRSA), Paris, France;

[b]Inovarion, Paris, France;

[c]Oncology Program, CIBEREHD, National Biomedical Research Institute on Liver and Gastrointestinal Diseases, Instituto de Salud Carlos III, Madrid, Spain; TGF-β and Cancer Group, Oncobell Program, Bellvitge Biomedical Research Institute (IDIBELL), Barcelona, Spain;

[d] LPP (Laboratoire de physique des plasmas, UMR 7648), Sorbonne Université, Centre national de la recherche scientifique (CNRS), Ecole Polytechnique, 75005 Paris, France;

[e]Assistance Publique-Hôpitaux de Paris (AP-HP) Sorbonne Université, Hôpital St Antoine, Paris, France;

[f]AP-HP, Reference Center for Inflammatory Biliary Diseases and Autoimmune Hepatitis (CRMR, MIVB-H), Department of Hepatology, Saint-Antoine Hospital, Paris, France.

Ester Gonzalez-Sanchez (ester.glezsan@gmail.com), Haquima El Mourabit (haquima.el-mourabit@inserm.fr), Marion Jager (marion.jager@hotmail.fr), Marie Clavel (marie.clavel@inovarion.com), Sophie Moog (sophie.moog@inovarion.com), Javier Vaquero (jvaquero@idibell.cat), Tatiana Ledent (tatiana.ledent@gmail.com), Axelle Cadoret (axelle.cadoret@inserm.fr), Jérémie Gautheron (jeremie.gautheron@inserm.fr), Laura Fouassier (laura.fouassier@inserm.fr), Dominique Wendum (dominique.wendum@aphp.fr), Nicolas Chignard (nicolas.chignard@inovarion.com), Chantal Housset (chantal.housset@inserm.fr).

*__Corresponding authors:__

Chantal Housset, M.D., Ph.D.

Sorbonne Université, Faculté de Médecine, Site Saint-Antoine, 27 rue Chaligny, 75571 Paris cedex 12, France. E-mail: chantal.housset@inserm.fr; Phone: (33) 1-40-01-13-59

Ester Gonzalez-Sanchez, Ph.D.
TGF-Beta and Cancer Group, IDIBELL,Gran Via de L'Hospitalet, 199, 08908 Barcelona, Spain. E-mail: ester.glezsan@gmail.com; Phone: (34) 932607429

[#]These authors share senior authorship

[1]Ester Gonzalez-Sanchez and Javier Vaquero are currently affiliated to Oncology Program, CIBEREHD, National Biomedical Research Institute on Liver and Gastrointestinal Diseases, Instituto de Salud Carlos III, Madrid, Spain; TGF-β and Cancer Group, Oncobell Program, Bellvitge Biomedical Research Institute (IDIBELL), Barcelona, Spain.

Abbreviations: ABCB4, ATP-binding cassette transporter B4; PSC, primary sclerosing cholangitis; VDR, vitamin D receptor; PDIA3, protein disulfide-isomerase A3; ERp57, endoplasmic reticulum protein 57; IPSCSG, International Primary Sclerosing Cholangitis Study Group; AST, aspartate aminotransferase; ALP, alkaline phosphatase; CK19, cytokeratin 19; TNFα, tumor necrosis factor α; HPRT1, hypoxanthine phosphoribosyltransferase 1; GAPDH, glyceraldehyde 3-phosphate dehydrogenase; VCAM1, vascular cell adhesion molecule 1; CCL, C-C motif chemokine ligand; MMP9, matrix metalloproteinase 9; CCR, C-C motif chemokine receptor.

ABSTRACT

Background & Aims: Cholangiopathies are chronic liver diseases in which damaged cholangiocytes trigger a proinflammatory and profibrotic reaction. The nuclear vitamin D receptor (VDR) is highly expressed in cholangiocytes and exerts immune-regulatory functions in these cells. In the present study, we examined the protective function of VDR and other vitamin D signaling pathways in chronic cholangiopathy and cholangiocytes.

Methods: *Vdr* was invalidated in *Abcb4* knockout mice, a widely used animal model of chronic cholangiopathy. The impact of vitamin D signaling on cholangiopathy features was examined *in vivo* and in cholangiocytes (primary and cell lines).

Results: Cholangiopathy features (*i.e*, cholestasis, ductular reaction and fibrosis) were aggravated in *Vdr;Abcb4* double knockout mice compared to the *Abcb4* simple knockout, and associated with an overexpression of proinflammatory factors. The proinflammatory phenotype of cholangiocytes was also exacerbated following VDR silencing *in vitro*. The expression of proinflammatory factors and the severity of cholangiopathy were reduced in the double knockout mice treated with the vitamin D analog calcipotriol or with vitamin D. *In vitro*, the inflammatory response to TNFα was significantly reduced by calcipotriol in biliary cells silenced for VDR, and this effect was abolished by co-silencing the plasma membrane receptor of vitamin D, protein disulfide-isomerase A3 (PDIA3).

Conclusions: Our results demonstrate an anti-inflammatory role of VDR signaling in cholangiocytes and cholangiopathy. They also provide evidence for PDIA3-mediated anti-inflammatory effects of vitamin D and vitamin D analog in these settings.

Keywords: Cholangiocyte; Cholestasis; Ductular reaction; Liver fibrosis; Protein disulfide-isomerase A3.

1. INTRODUCTION

Cholangiopathies are chronic liver diseases in which damaged cholangiocytes trigger a proinflammatory and profibrotic response, that leads to the development of cirrhosis and end-stage liver disease [1]. Vitamin D deficiency is common in chronic liver diseases, and it is associated with increased liver inflammation and fibrosis [2-5]. It has also been reported that vitamin D deficiency is associated with an aggravation of liver fibrosis in a model of chronic cholangiopathy [6] that mimics primary sclerosing cholangitis (PSC), *i.e.*, the ATP-binding cassette transporter B4 (*Abcb4*) knockout mouse model [7-10]. Currently there are two vitamin D receptors described to mediate the biological effects of vitamin D. The nuclear receptor, vitamin D receptor (VDR), is the best characterized of these receptors. A membrane-associated receptor of vitamin D, protein disulfide-isomerase A3 (PDIA3) also known as endoplasmic reticulum protein 57 (ERp57), has also been described [11]. While PDIA3 elicits non-genomic responses, VDR mediates the biological effects of vitamin D by modulating the transcription of target genes. Especially, VDR mediates anti-inflammatory and anti-fibrotic effects of vitamin D through gene regulation. Of particular interest with respect to cholangiopathies, VDR expression is restricted to non-parenchymal cells in the liver, and largely predominant in cholangiocytes [12, 13], implying direct actions of VDR in cholangiocytes and cholangiopathies. Furthermore, VDR gene variations have been associated with auto-immune biliary diseases [14]. We previously showed that VDR promoted innate immunity in cholangiocytes [15] and that the absence of VDR altered the biliary epithelial cell barrier function leading to an aggravated phenotype of acute cholestatic liver injury in the mouse model of bile duct ligation [16]. We also showed that VDR expression in cholangiocytes was increased in the *Abcb4* knockout mice [13], suggesting an activation

of VDR signaling in a chronic setting of cholangiopathy. Moreover, other ligands such as bile acids may account for VDR protective effects in the liver [15].

In the present study we tested the protective function of VDR in chronic cholangiopathy by inactivating VDR in the *Abcb4* knockout mouse model and we also evaluated the potential of vitamin D and vitamin D analog to exert VDR-independent effects in this model and in cholangiocyte cell models.

2. MATHERIALS AND METHODS

2.1. Animal experiments

Abcb4 simple knockout mice and their wildtype littermates were bred, using *Abcb4*$^{+/-}$ heterozygous mice on an FVB/N genetic background (FVB.129P2-Abcb4tm1Bor/J) provided by Sanofi R&D (Chilly-Mazarin, France). To develop *Vdr*;*Abcb4* double knockout congenic mice, first we generated *Vdr*$^{+/-}$ mice on an FVB/N background. *Vdr*$^{+/-}$ mice on a C57BL/6J background (B6.129S4-Vdr^{tm1Mbd}/J) from Charles River Laboratories (Wilmington, MA, USA), were backcrossed with wildtype FVB/N mice (Charles River Laboratories) for 5 generations, using a speed congenics protocol. Next, *Vdr*$^{+/-}$ and *Abcb4*$^{-/-}$ mice on a FVB/N background were crossed to generate *Vdr*$^{+/-}$;*Abcb4*$^{-/-}$ mice, which were further crossed to obtain *Vdr*$^{+/+}$;*Abcb4*$^{-/-}$ and *Vdr*$^{-/-}$;*Abcb4*$^{-/-}$ mice (Supplementary Figure S1 A-B). Wildtype mice used as a reference in the study, were all on a FVB/N background. Mice were housed at CRSA animal facility (Institutional Animal Care and Use Direction, DDPP agreement No. C 75-12-01), in a temperature-controlled, specific pathogen-free environment, on a 12-hour light-dark cycle, with free access to a standard chow containing 1.2 IU vitamin D/kg (LASQCdiet® Rod16-R, Genobios, Laval, France) and water. All investigations were performed in males. During housing, animals were monitored daily for healthy status. Sub-groups of mice received intraperitoneal injections of 40 µg/kg calcipotriol (Tocris, Bristol, UK), 3 times a week, an optimal dose to produce beneficial effects according to a previous report [17], from the age of 4 weeks to 8 weeks, or long-term vitamin D dietary supply, in which case, mice were fed a diet containing 2.2 IU vitamin D/kg, enriched in calcium and phosphate (TD96348, Envigo, Huntington, UK) [16] after weaning at 4 weeks, until the

age of <u>12 months.</u> Mice were included in lifespan studies or sacrificed under isoflurane anesthesia, at different time points. Upon sacrifice, blood was withdrawn from the vena cava and the liver and spleen were collected and weighed. Liver samples were harvested following recommendations from the International Primary Sclerosing Cholangitis Study Group (IPSCSG) [10]. In a sub-set of experiments, cholangiocytes and different liver cell types were isolated from 8 week-old mice, using an *in situ* perfusion-based protocol, as previously described [13]. All experiments complied with the European Directive 2010/63/UE and the ARRIVE Guidelines, and were approved by the Ethics Committee of Animal Experiments, Charles Darwin No.5 (No. APAFIS#364-2015032410575237v3 and APAFIS#16333-2018072719352187v1).

2.2. Biochemistry

The concentrations of aspartate and alanine aminotransferases, alkaline phosphatase (ALP) total bilirubin, <u>calcium and phosphate</u> in plasma, were measured on an Olympus AU400 Analyzer. Bile acid concentrations in plasma were determined using the Bile Acid Kit Ecoline S+ (DiaSys Diagnostic Systems GmbH, Holzheim, Germany) on a Hitachi917 analyzer. Hydroxyproline content in liver tissue was measured in lobe 3, using a colorimetric kit from Sigma-Aldrich (Saint-Louis, MO, USA), as previously described [18].

2.3. Histology and (immuno)histochemistry

Formalin (4%)-fixed, paraffin-embedded, mouse and human liver tissue samples were cut into 4-μm-thick sections. Mouse liver tissue sections were stained with hematoxylin and eosin or Sirius red, or were immunostained for cytokeratin 19 (CK19) or <u>F4/80</u>, using an anti-CK19 antibody (TROMA III, Developmental Studies Hybridoma Bank, Iowa University, IA, USA), <u>and an anti-F4/80 antibody (SP115, Abcam, Cambridge, UK),</u> <u>respectively,</u> as described [19, 20]. Stained sections were scanned on a virtual slide

scanner (Hamamatsu, Tokyo, Japan) 2.0 HT, using a 3-charge-coupled device, time-delay integration camera with a resolution of 1.84 µm/pixel (x20 objective) and 0.92 µm/pixel (x40 objective). Morphometric analyses were performed blinded, using ImageJ analysis software (National Institutes of Health, Bethesda, MD, USA). Paraffin-embedded human liver samples stored in the Pathological Department of Saint-Antoine Hospital were provided by this Department. Normal liver sample was from a patient who underwent liver surgery for tumor and pathological liver from a patient with PSC who underwent liver surgery for gallbladder carcinoma. Human liver tissue sections were immunolabeled for PDIA3. First, they were incubated in sodium citrate pH 6, for 20 min at 95°C, to unmask epitopes, and then with 3% bovine serum albumin, to block unspecific binding. Thereafter, sections were incubated with PDIA3 antibody (CL2444, Sigma-Aldrich) diluted 1/100 in Envision flex diluent (Agilent Technologies, Santa Clara, CA, USA), overnight at 4°C. Sections were then incubated with a secondary anti-mouse antibody coupled to Alexa fluor 488 (Invitrogen/Thermo Fisher Scientific, Walthman, MA, USA) diluted 1/200 in 3% bovine serum albumin, at room temperature for one hour. Nuclear staining was performed, using DRAQ5 (Abcam) at 1/1000, for 5 min at room temperature. Tissue sections were examined with a SP2 confocal microscope (Leica, Bannockburn, IL, USA).

2.4. *In vitro* studies

The human biliary epithelial cells Mz-ChA-1 and EGI-1 were obtained from Dr. A. Knuth (Zurich University, Switzerland) and from the German Collection of Microorganisms and Cell Cultures (DSMZ, Braunschweig, Germany), respectively. Although derived from tumor cells, these cell lines can be phenotypically similar to primary biliary epithelial cells [21], and have been validated as surrogate models of cholangiocytes in different settings, including cholestatic liver injury [15, 16, 22-25]. Both Mz-ChA-1 and EGI-1

cells were cultured in DMEM supplemented with 1 g/L glucose, 10 mmol/L HEPES, 10% fetal bovine serum, 100 IU/mL penicillin, 100 µg/mL streptomycin, 0.25 µg/mL amphotericin B (Thermo Fisher Scientific). For transient transfection experiments, Mz-ChA-1 and EGI-1 cells were seeded into 6-well plates (250,000 and 140,000 cells/well, respectively). Cells were transfected with ON-TARGETplus human VDR or PDIA3 siRNA SMARTpools, or siGENOME Non-Targeting siRNA (Horizon Discovery LTD, Cambridge, UK) using DarmaFECT 4 (Horizon Discovery LTD). Seventy-two hours after transfection, cells were incubated with serum-free medium for 12 hours and then treated with tumor necrosis factor (TNF) α (10 ng/mL; Sigma-Aldrich), as previously described [25, 26], combined with calcipotriol (100 nmol/L) [27] or vehicle (DMSO) for 24 hours. Cell lines were routinely screened for the presence of mycoplasma and authenticated for polymorphic markers to prevent cross-contamination.

2.5. Reverse transcription quantitative PCR (RT-qPCR)

Total RNA was extracted using RNeasy columns (Qiagen, Courtaboeuf, France). Complementary DNA was synthesized from total RNA (l µg), using the SuperScript II Reverse Transcriptase (Thermo Fisher Scientific), and qPCR was performed using the Sybr Green Master Mix, on a Light-Cycler 96 (Roche Diagnostics, Basel, Switzerland). Primer sequences are provided in Supporting Table S1. The mRNA levels of target genes were normalized for those of hypoxanthine phosphoribosyltransferase 1 (*Hprt1*) in mouse or glyceraldehyde 3-phosphate dehydrogenase (*GAPDH*) in human, and expressed as relative levels ($2^{-\Delta\Delta Ct}$).

2.6. Immunoblot

Proteins were extracted from liver or colon tissue, separated by 10% SDS-PAGE and transferred to nitrocellulose membranes. Membranes were incubated with primary antibodies raised against PDIA3 (1/2000; ab10287 Abcam), VDR (1/200; sc-13133 Santa

Cruz, Dallas, TX, USA), GAPDH (1/5000; sc-32233 Santa Cruz) or β-Actin (1/2000, A5441 Sigma-Aldrich), overnight at 4°C, and then with secondary, horseradish peroxidase-conjugated antibodies raised against mouse or rabbit IgG (1/2000; Cell Signaling-Ozyme, Saint-Quentin en Yveline, France), for 1 hour at room temperature. Bound antibodies were revealed by enhanced chemiluminescence (Thermo Fischer Scientific). Blots were visualized using ChemiDoc^{TM} Touch Imaging System (BioRad, Hercules, CA, USA) and densitometric analysis was performed using Image Lab^{TM} Software (BioRad).

2.7. Statistics

Data are expressed as mean ± standard deviation, SD. Statistical analyses were performed using GraphPad Prism software version 5.0 (GraphPad Software San Diego, CA, USA). For comparisons between two groups, Mann-Whitney nonparametric *U* test and Student's *t* test were used. Differences between more than two groups were assed using the nonparametric Kruskall-Wallis test followed by Dunn's multiple comparison or one-way ANOVA with Bonferroni post-hoc test. Log-rank test was used to compare Kaplan–Meier survival curves. A *P* value of less than 0.05 was considered significant. Each figure legend states number of experiments performed (*n*), and the statistical test applied.

3. RESULTS

3.1. VDR ablation causes a reduction of lifespan and an increase in the severity of liver injury in *Abcb4* knockout mice

Double knockout ($Vdr^{-/-};Abcb4^{-/-}$) mice were generated and monitored in comparison with simple knockout ($Vdr^{+/+};Abcb4^{-/-}$) littermates, for up to 12 months. $Vdr^{-/-};Abcb4^{-/-}$ mice were viable and showed no overt phenotypic difference with $Vdr^{+/+};Abcb4^{-/-}$ littermates at birth. During follow-up, they showed moderate hypocalcemia compared to $Vdr^{+/+};Abcb4^{-/-}$, whereas the plasma concentrations of phosphate, although transiently lower than in the $Vdr^{+/+};Abcb4^{-/-}$, remained above normal levels (Supplementary Figure S1 C-D). Noticeably, lifespan was significantly reduced in $Vdr^{-/-};Abcb4^{-/-}$ mice as compared to $Vdr^{+/+};Abcb4^{-/-}$ mice, and did not exceed 11 months in these animals (Figure 1A).

To evaluate the impact of *Vdr* invalidation on liver phenotype in $Abcb4^{-/-}$ mice, we performed comparative analyses of liver disease features in $Vdr^{-/-};Abcb4^{-/-}$ and $Vdr^{+/+};Abcb4^{-/-}$ mice at the age of 2 weeks, 4 weeks, 8 weeks and 6 months. Macroscopic examination showed that, compared to simple knockout mice, $Vdr^{-/-};Abcb4^{-/-}$ mice developed more severe hepatomegaly and splenomegaly (Figure 1B). Histological analysis was performed using an adaptation (described in Supplementary Materials and Methods) of Nakamuna scoring [28]. According to this analysis, cholangitis and fibrosis appeared to be more pronounced in $Vdr^{-/-};Abcb4^{-/-}$ mice than in age-matched $Vdr^{+/+};Abcb4^{-/-}$ littermates from 8 weeks on (Figure 1C & Supplementary Table S2).

$Vdr^{-/-};Abcb4^{-/-}$ mice also displayed a rise in the plasma levels of alanine aminotransferase (ALT) (not shown) and aspartate aminotransferase (AST), which from 4 weeks on, were 1.5 to 2.5 higher than those observed in $Vdr^{+/+};Abcb4^{-/-}$ mice (Figure 1D). The plasma levels of ALP also rose to a greater extent in $Vdr^{-/-};Abcb4^{-/-}$ mice than in $Vdr^{+/+};Abcb4^{-/-}$ mice from 4 weeks on, as did those of total bilirubin and bile acids from 8 weeks on (Figure 1D). Taken together these results indicated that $Vdr^{-/-};Abcb4^{-/-}$ mice developed more severe cholestatic liver injury than $Vdr^{+/+};Abcb4^{-/-}$ mice.

3.2. VDR ablation causes an aggravation of cholangiopathy features in *Abcb4* knockout mice

Ductular reaction, which is characterized by a proliferative response of cholangiocytes to injury, is a hallmark of cholangiopathies. We performed CK19 immunostaining on liver tissue sections to assess ductular reaction in the simple and double knockout mice. As previously reported in the *Abcb4* simple knockout mice [29], ductular reaction reached its maximal point both in $Vdr^{+/+};Abcb4^{-/-}$ and $Vdr^{-/-};Abcb4^{-/-}$ mice at the age of 8 weeks, and became less prominent from this point on (Figure 2A). Both at 8 weeks and 6 months, the ductular reaction was significantly more <u>pronounced</u> in $Vdr^{-/-};Abcb4^{-/-}$ mice than in $Vdr^{+/+};Abcb4^{-/-}$ mice (Figure 2A). Thus reactive cholangiocytes were more abundant in $Vdr^{-/-};Abcb4^{-/-}$ mice than in $Vdr^{+/+};Abcb4^{-/-}$ mice.

Reactive cholangiocytes contribute to liver inflammation in cholangiopathies by releasing pro-inflammatory mediators. Therefore, we next assessed the expression of pro-inflammatory factors that are typically produced by reactive cholangiocytes in cholangiopathies in both groups of mice. At the peak time of ductular reaction, *i.e.*, 8

weeks, pro-inflammatory factors including *Tnfα*, vascular cell adhesion molecule 1 (*Vcam1*), C-C motif chemokine ligand (*Ccl*)2, *Ccl20*, *S100a8*, *S100a9* and matrix metalloproteinase 9 (*Mmp9*) were overexpressed in the liver of both $Vdr^{+/+};Abcb4^{-/-}$ and $Vdr^{-/-};Abcb4^{-/-}$ mice, as shown relative to wildtype mice. Importantly, all these genes were expressed at higher levels in $Vdr^{-/-};Abcb4^{-/-}$ mice than in $Vdr^{+/+};Abcb4^{-/-}$ mice (Figure 2B). The overexpression of *Ccl2* and *Ccl20*, which play an essential role in the recruitment of circulating monocytes to injured tissues, was accompanied by an overexpression of their receptors, *i.e.*, CC chemokine receptor *(Ccr)2* and *Ccr6*, respectively (Supplementary Figure S2). Consistent with these results, macrophages were more abundant in the liver of $Vdr^{-/-};Abcb4^{-/-}$ mice than in $Vdr^{+/+};Abcb4^{-/-}$ mice, as ascertained by F4/80 immunostaining (Figure 2C). Altogether these results attested an exacerbation of the immune response in the liver of $Abcb4^{-/-}$ mice in the absence of VDR.

Proinflammatory chemokines and cytokines overproduced in the liver are expected to stimulate liver myofibroblasts and promote liver fibrosis. The quantification of hepatic hydroxyproline content indicated that more collagen accumulated in the liver of $Vdr^{-/-};Abcb4^{-/-}$ mice compared to single knockout mice (Figure 2D, right lower panel). In line with this observation, Sirius red staining showed more extensive liver fibrosis in $Vdr^{-/-};Abcb4^{-/-}$ mice than in $Vdr^{+/+};Abcb4^{-/-}$ mice (Figure 2D, upper, and left lower panels). In agreement with a previous report [30], we observed a stabilization of the liver phenotype in the $Abcb4^{-/-}$ mice (on FVB/N background) with no further aggravation after 8 weeks, and this was true irrespective of the VDR status.

Collectively, these findings indicate that in the absence of VDR, ductular reaction, pro-inflammatory signals and collagen deposition were amplified in the liver of $Abcb4^{-/-}$ mice, highlighting a protective action of VDR in the setting of chronic cholangiopathy.

3.3. Calcipotriol treatment reverses the aggravation of cholangiopathy features in $Vdr^{-/-};Abcb4^{-/-}$ mice

To gain further insights into the protection that vitamin D signaling might confer in the setting of cholangiopathies, we administered a 4-week treatment with calcipotriol, a synthetic vitamin D analog, both in $Vdr^{+/+};Abcb4^{-/-}$ and $Vdr^{-/-};Abcb4^{-/-}$ mice. At the end of treatment, no significant change in blood tests of cholestatic liver injury was observed either in $Vdr^{+/+};Abcb4^{-/-}$ or $Vdr^{-/-};Abcb4^{-/-}$ mice. However, the ductular reaction assessed by CK19 immunostaining was significantly reduced following calcipotriol treatment in $Vdr^{-/-};Abcb4^{-/-}$ mice, whereas it remained unchanged in the $Vdr^{+/+};Abcb4^{-/-}$ mice (Figure 3B). Calcipotriol treatment also elicited a significant decrease in the expression of $Tnf\alpha$, $Ccl2$, $Ccl20$, $S100a8$, $S100a9$ and $Mmp9$ in the liver of $Vdr^{-/-};Abcb4^{-/-}$ mice while no effect on the expression of these factors was found in the liver of $Vdr^{+/+};Abcb4^{-/-}$ mice (Figure 3C). Accordingly, the inflammatory infiltrate assessed by F4/80 immunostaining was reduced in calcipotriol-treated $Vdr^{-/-};Abcb4^{-/-}$ mice compared to the untreated mice (Figure 3D), and fibrosis less severe as shown by a significant difference in hydroxyproline content (Figure 3E). By contrast, calcipotriol treatment had no such effects in $Vdr^{+/+};Abcb4^{-/-}$ mice (Figure 3D). Overall, while calcipotriol treatment did not stop the progression of liver disease in $Vdr^{+/+};Abcb4^{-/-}$ mice, it improved liver

status and reversed the aggravation of cholangiopathy features in $Vdr^{-/-};Abcb4^{-/-}$ mice. This indicated that the vitamin D analog activated a VDR-independent pathway that attenuated the severity of cholangiopathy in the double knockout mice.

3.4. PDIA3 is overexpressed in the liver and cholangiocytes of $Vdr^{-/-};Abcb4^{-/-}$ mice

PDIA3, the membrane receptor of vitamin D, mediates anti-inflammatory actions by mechanisms such as the ectodomain shedding of TNF receptor 1 [31, 32]. We hypothesized that the VDR-independent effects of calcipotriol observed in $Vdr^{-/-};Abcb4^{-/-}$ mice, could be mediated by PDIA3. Consistent with this hypothesis, we found that hepatic *Pdia3* mRNA and protein expression was significantly increased in $Vdr^{-/-};Abcb4^{-/-}$ mice compared to wildtype (FVB/N) and $Vdr^{+/+};Abcb4^{-/-}$ mice (Figure 4, A and B). Looking into pools of individual liver cell types that were isolated from wildtype and simple *Abcb4* knockout mice, we found that they all expressed *Pdia3*, but that *Pdia3* expression increased distinctively in cholangiocytes from *Abcb4* knockout mice compared to wildtype, whereas little change occurred in the other cell types (Figure 4C). We also examined *Pdia3* expression specifically in cholangiocytes from $Vdr^{-/-};Abcb4^{-/-}$ mice, and found an even higher expression than in the simple knockout and wildtype mice (Figure 4D). Because cholangiocytes i) are more numerous and ii) express more *Pdia3* in the liver of $Vdr^{-/-};Abcb4^{-/-}$ mice than in the wildtype and simple *Abcb4* knockout mice, we inferred that they accounted at least partly for *Pdia3* overexpression in the liver of the double knockout. We could also show that in the liver tissue from a patient with PSC, PDIA3 was immunodetected in cholangiocytes of both small and large bile ducts and localized at their plasma membrane where it could mediate vitamin D effects (Figure 4E). Moreover, the intensity of labeling in cholangiocytes appeared to be higher in PSC than

in normal liver (Figure 4E). Collectively, our results indicated that cholangiocytes are a major site of PDIA3 expression in cholangiopathy.

3.5. PDIA3 mediates VDR-independent anti-inflammatory effects of calcipotriol in cholangiocytes

To examine whether PDIA3 in cholangiocytes could contribute to VDR-independent effects of calcipotriol in $Vdr^{-/-};Abcb4^{-/-}$ mice, we invalidated VDR and PDIA3 in human cholangiocytes. Two human biliary epithelial cell lines, Mz-ChA-1 and EGI-1, commonly studied as surrogate models of non-tumoral human cholangiocytes [15, 16, 21-25], were transfected with $VDR \pm PDIA3$ siRNA (Supplementary Figure S3, A and B). VDR knockdown caused a significant increase in the expression of pro-inflammatory factors that were found to be overexpressed in the liver of $Vdr^{-/-};Abcb4^{-/-}$ mice, including $CCL2$, $CCL20$, $S100A9$ and $MMP9$ in MzChA-1 cells (Figure 5A), and $CCL20$, $S100A9$ and $MMP9$ in EGI-1 (Supplementary Figure S4A). Similar variations of these factors were observed in cholangiocytes isolated from the double compared to simple knockout mice, even though only the difference in $Ccl20$ expression reached statistical significance (Supplementary Figure S5). VDR knockdown also caused a significant increase in PDIA3 in human biliary epithelial cell lines (Supplementary Figure S3, A and B). Next, we tested the effect of calcipotriol in the context of cholangiocyte inflammatory response to TNFα [25, 26]. TNFα induced a marked increase in the expression of $CCL2$, $CCL20$, $S100A9$ and $MMP9$ in Mz-ChA-1 cells (Figure 5B). Calcipotriol significantly reduced the rise triggered by TNFα in the expression of $CCL2$, $CCL20$ and $MMP9$ in these cells (Figure 5B). The inhibitory effect of calcipotriol was also observed in the cells silenced for VDR, whereas no such effect occurred in the cells silenced for both VDR and PDIA3 (Figure 5B). EGI-1 cells also displayed an overexpression of $CCL20$, $S100A9$ and $MMP9$, when silenced for VDR (Supplementary Figure S4A). Although they were poorly

responsive to TNFα in basal conditions, the overexpression of *S100A9* and *MMP9* induced by TNFα was reduced by calcipotriol in cells lacking VDR, but not in those lacking both VDR and PDIA3 (Supplementary Figure S4B). Taken together, these results indicated that in the absence of VDR, PDIA3 mediated anti-inflammatory effects of calcipotriol in the liver, which may have contributed to the protective effects of calcipotriol observed in *Vdr*$^{-/-}$;*Abcb4*$^{-/-}$ mice.

3.6. Long-term vitamin D supplementation alleviates the severity of cholangiopathy phenotype in *Vdr*$^{-/-}$;*Abcb4*$^{-/-}$ mice

To further confirm that vitamin D can elicit VDR-independent protective mechanisms in cholangiopathy, we tested long-term natural vitamin D supplementation in the *Abcb4* knockout mice. *Vdr*$^{+/+}$;*Abcb4*$^{-/-}$ and *Vdr*$^{-/-}$;*Abcb4*$^{-/-}$ mice were fed a vitamin D-enriched diet from weaning until the age of 6 months. Akin to short-term pharmacological treatment with calcipotriol, long-term vitamin D supplementation improved cholangiopathy features in *Vdr*-invalidated *Abcb4* knockout mice. Cholestasis, ductular reaction and liver fibrosis were all significantly less intense in the double knockout mice who received vitamin D supplementation for 6 months compared to those who were fed a regular chow diet (Figure 6, A-C). By contrast, no improvement resulted from vitamin D supplementation in the *Vdr*$^{+/+}$;*Abcb4*$^{-/-}$ mice even though we observed a significant reduction of ALP levels which might reflect an improvement by vitamin D supplementation of the hepatic osteodystrophy that occurs in *Abcb4*$^{-/-}$ mice [33].

Consistent with these results, long-term vitamin D supplementation improved survival rates only in *Vdr*$^{-/-}$;*Abcb4*$^{-/-}$ mice (Figure 6D). These results confirmed the existence of

an alternative vitamin D signaling pathway independent of VDR, which promotes protective mechanisms in cholangiopathy.

4. DISCUSSION

In this study, we demonstrate the protective functions of VDR in a mouse model of chronic cholangiopathy. Cholestasis, hepatic inflammation and fibrosis were exacerbated by the loss of VDR in *Abcb4* knockout mice. Yet, the activation of VDR by vitamin D or calcipotriol treatments failed to ameliorate cholangiopathy in *Abcb4* knockout mice. Instead, vitamin D and calcipotriol treatments improved liver injury in the *Abcb4* knockout mice that lacked VDR, implying the existence of VDR-independent protective effects of vitamin D and analog in this model. Our data provide evidence to indicate that VDR-independent actions of vitamin D in this context may be mediated by PDIA3.

Biochemical markers of liver injury and inflammation were increased in *Abcb4* knockout mice in the absence of VDR. *Vdr* knockout mice on a C57BL/6J background spontaneously develop hepatic inflammation and fibrosis at the age of 6 months [27, 34]. These observation have been attributed to anti-inflammatory and anti-fibrotic effects of VDR in liver macrophages [34] and hepatic stellate cells [27], respectively. Without excluding that these effects contributed to the development of a more severe liver phenotype in $Vdr^{-/-};Abcb4^{-/-}$ mice compared to $Vdr^{+/+};Abcb4^{-/-}$, we herein specifically addressed the contribution of *Vdr* loss in cholangiocytes. The first reason is that VDR expression in the liver, is most prominent in cholangiocytes than in any other liver cell type, both in humans [15] and in mice, especially in the context of chronic cholangiopathy, as shown in *Abcb4* knockout mice [13]. The second reason is that cholangiocytes are proliferative and produce pro-inflammatory factors in cholangiopathies, whereby they promote fibrosis and disease progression in these disorders [1]. We found that cholangiocytes lacking VDR overexpressed pro-inflammatory factors both *in vivo* and *in vitro*. Moreover, cholangiocytes lacking VDR were more proliferative *in vivo* (Figure 2A), suggesting that cholangiocytes played a

significant role in the aggravation of cholangiopathy caused by VDR loss. While VDR has been shown to promote epithelial barrier integrity [16, 35], we could not detect more bile duct disruption in $Vdr^{-/-}$ mice than in $Vdr^{+/+}$ mice in the chronic model of $Abcb4$ invalidation (Supplementary Figure S6). Neither did we detect a significant increase in the permeability or histology of the intestine of $Vdr^{-/-};Abcb4^{-/-}$ compared to $Vdr^{+/+};Abcb4^{-/-}$ mice (Supplementary Figure S7).

Activation of VDR by vitamin D analogs has been considered as a therapeutic option in chronic liver diseases. Supporting this strategy, hypocalcemic vitamin D analogs approved for use in patients (*i.e.* calcipotriol, for topical treatments; alfacalcidol and paricalcitol for systemic treatments), have demonstrated antifibrotic properties both in hepatic stellate cells *in vitro* [27, 36], and in mouse models of CCl$_4$- and- thioacetamide-induced liver fibrosis *in vivo* [27, 36, 37]. Calcipotriol used as a prophylactic treatment has also been shown to prevent biliary fibrosis induced by bile duct ligation or 3,5-diethoxycarbonyl-1,4-dihydrocollidine (DDC) in mice [38]. However, when used as a curative treatment, calcipotriol herein failed to improve liver fibrosis in *Abcb4* knockout mice. Liver fibrosis in *Abcb4* knockout mice was left unchanged by treatments with active vitamin D (calcitriol), or a high-dose vitamin D diet, as shown here and in a previous study [6, 39]. Yet, *Abcb4* knockout mice on low vitamin D diet display aggravated liver fibrosis, which in this particular case, can be ameliorated by a vitamin D-sufficient diet [6]. Importantly, in such case, a high vitamin D supplementation adds no benefit over a normal intake [6]. Taken together, these data indicate that normal levels of vitamin D are sufficient to ensure VDR-dependent protective mechanisms in cholangiopathies. They suggest that in a setting of effective VDR signaling, increasing VDR ligands does not provide further therapeutic benefit.

Remarkably, we found that both high-dose vitamin D supplementation and a vitamin D analog were beneficial in *Abcb4* knockout mice lacking VDR, highlighting VDR-independent protective effects of vitamin D. We postulated that VDR-independent protective effects of vitamin D and analogs in the liver, could be mediated by PDIA3, the membrane receptor of vitamin D [11]. Consistent with this assumption, we could show that PDIA3 was expressed at high levels in cholangiocytes of *Abcb4* knockout mice. Furthermore, pro-inflammatory response was suppressed by calcipotriol acting *via* PDIA3 in cholangiocytes, as demonstrated *in vitro*. In keeping with this result, PDIA3 was previously shown to mediate nongenomic actions of vitamin D by shedding the ectodomain of TNF receptor 1, thus decreasing responsiveness to TNFα [31]. Noteworthily, this mechanism is activated by Vitamin D3 and derivatives [32], to which calipotriol belongs. The binding potency of vitamin D for PDIA3 is lower than for VDR [40], suggesting that vitamin D or calcipotriol preferentially bind to VDR in cells that express both receptors. Therefore, we suggest that PDIA3 mediates anti-inflammatory effects of vitamin D particularly in the context of defective VDR signaling, when the ligand bioavailability is increased and PDIA3 overexpressed, as shown here and in a previous study [41]. Nevertheless, specific ligands of this receptor are currently lacking and need to be developed to further explore the role of PDIA3 in the inflammatory response of cholangiocytes.

The clinical relevance of our findings is supported by previous studies showing that in subjects with liver disease, VDR gene variants can lead to low VDR expression in the liver, which is associated with a higher severity of inflammation and fibrosis [42, 43]. Therefore, while a treatment aimed to maintain normal levels of vitamin D may be sufficient in a large number of patients with cholangiopathies, a subset of patients could benefit from Vitamin D treatments *via* PDIA3. Further studies are needed to determine

the impact of VDR polymorphisms on disease progression (prognosis, severity or risk of cancer development) in patients with cholangiopathies. This may help to identify subgroup of patients that would benefit from treatments with supra-physiological doses of vitamin D. Furthermore, additional strategies aimed to boost PDIA3 anti-inflammatory effects with PDIA3-specific ligands may be of clinical interest regardless of VDR expression status. The present study provides rationale to explore this strategy in the future.

In conclusion, the present findings provide new mechanistic insights into the involvement of vitamin D signaling in cholangiocytes and cholangiopathies. They indicate that the VDR status of patients with cholangiopathies may be as important as circulating vitamin D levels in these diseases. Moreover, our data provide evidence for PDIA3 anti-inflammatory effects in cholangiocytes, suggesting a potential interest as a therapeutic target in cholangiopathies.

REFERENCES

[1] J.M. Banales, R.C. Huebert, T. Karlsen, M. Strazzabosco, N.F. LaRusso, G.J. Gores, Cholangiocyte pathobiology, Nat Rev Gastroenterol Hepatol, 16 (2019) 269-281.

[2] S. Petta, C. Camma, C. Scazzone, C. Tripodo, V. Di Marco, A. Bono, D. Cabibi, G. Licata, R. Porcasi, G. Marchesini, A. Craxi, Low vitamin D serum level is related to severe fibrosis and low responsiveness to interferon-based therapy in genotype 1 chronic hepatitis C, Hepatology, 51 (2010) 1158-1167.

[3] E. Trepo, R. Ouziel, P. Pradat, Y. Momozawa, E. Quertinmont, C. Gervy, T. Gustot, D. Degre, V. Vercruysse, P. Deltenre, L. Verset, B. Gulbis, D. Franchimont, J. Deviere, A. Lemmers, C. Moreno, Marked 25-hydroxyvitamin D deficiency is associated with poor prognosis in patients with alcoholic liver disease, Journal of hepatology, 59 (2013) 344-350.

[4] T. Arai, M. Atsukawa, A. Tsubota, M. Koeda, Y. Yoshida, T. Okubo, A. Nakagawa, N. Itokawa, C. Kondo, K. Nakatsuka, T. Masu, K. Kato, N. Shimada, T. Hatori, N. Emoto, M. Kage, K. Iwakiri, Association of vitamin D levels and vitamin D-related gene polymorphisms with liver fibrosis in patients with biopsy-proven nonalcoholic fatty liver disease, Dig Liver Dis, 51 (2019) 1036-1042.

[5] A.J. Czaja, A.J. Montano-Loza, Evolving Role of Vitamin D in Immune-Mediated Disease and Its Implications in Autoimmune Hepatitis, Dig Dis Sci, 64 (2019) 324-344.

[6] K. Hochrath, C.S. Stokes, J. Geisel, M.J. Pollheimer, P. Fickert, S. Dooley, F. Lammert, Vitamin D modulates biliary fibrosis in ABCB4-deficient mice, Hepatol Int, 8 (2014) 443-452.

[7] T.H. Mauad, C.M. van Nieuwkerk, K.P. Dingemans, J.J. Smit, A.H. Schinkel, R.G. Notenboom, M.A. van den Bergh Weerman, R.P. Verkruisen, A.K. Groen, R.P. Oude Elferink, et al., Mice with homozygous disruption of the mdr2 P-glycoprotein gene. A novel animal model for studies of nonsuppurative inflammatory cholangitis and hepatocarcinogenesis, The American journal of pathology, 145 (1994) 1237-1245.

[8] P. Fickert, A. Fuchsbichler, M. Wagner, G. Zollner, A. Kaser, H. Tilg, R. Krause, F. Lammert, C. Langner, K. Zatloukal, H.U. Marschall, H. Denk, M. Trauner, Regurgitation of bile acids from leaky bile ducts causes sclerosing cholangitis in Mdr2 (Abcb4) knockout mice, Gastroenterology, 127 (2004) 261-274.

[9] Y. Popov, E. Patsenker, P. Fickert, M. Trauner, D. Schuppan, Mdr2 (Abcb4)-/- mice spontaneously develop severe biliary fibrosis via massive dysregulation of pro- and antifibrogenic genes, Journal of hepatology, 43 (2005) 1045-1054.

[10] P. Fickert, M.J. Pollheimer, U. Beuers, C. Lackner, G. Hirschfield, C. Housset, V. Keitel, C. Schramm, H.U. Marschall, T.H. Karlsen, E. Melum, A. Kaser, B. Eksteen, M. Strazzabosco, M. Manns, M. Trauner, P.S.C.S.G. International, Characterization of animal models for primary sclerosing cholangitis (PSC), Journal of hepatology, 60 (2014) 1290-1303.

[11] A. Hettinghouse, R. Liu, C.J. Liu, Multifunctional molecule ERp57: From cancer to neurodegenerative diseases, Pharmacol Ther, 181 (2018) 34-48.

[12] M. Gascon-Barre, C. Demers, A. Mirshahi, S. Neron, S. Zalzal, A. Nanci, The normal liver harbors the vitamin D nuclear receptor in nonparenchymal and biliary epithelial cells, Hepatology, 37 (2003) 1034-1042.

[13] E. Gonzalez-Sanchez, D. Firrincieli, C. Housset, N. Chignard, Expression patterns of nuclear receptors in parenchymal and non-parenchymal mouse liver cells and their modulation in cholestasis, Biochim Biophys Acta Mol Basis Dis, 1863 (2017) 1699-1708.

[14] A. Vogel, C.P. Strassburg, M.P. Manns, Genetic association of vitamin D receptor polymorphisms with primary biliary cirrhosis and autoimmune hepatitis, Hepatology, 35 (2002) 126-131.

[15] E. D'Aldebert, M.J. Biyeyeme Bi Mve, M. Mergey, D. Wendum, D. Firrincieli, A. Coilly, L. Fouassier, C. Corpechot, R. Poupon, C. Housset, N. Chignard, Bile salts control the antimicrobial peptide cathelicidin through nuclear receptors in the human biliary epithelium, Gastroenterology, 136 (2009) 1435-1443.

[16] D. Firrincieli, S. Zuniga, C. Rey, D. Wendum, E. Lasnier, D. Rainteau, T. Braescu, T. Falguieres, M. Boissan, A. Cadoret, C. Housset, N. Chignard, Vitamin D nuclear receptor deficiency promotes cholestatic liver injury by disruption of biliary epithelial cell junctions in mice, Hepatology, 58 (2013) 1401-1412.

[17] M.H. Sherman, R.T. Yu, D.D. Engle, N. Ding, A.R. Atkins, H. Tiriac, E.A. Collisson, F. Connor, T. Van Dyke, S. Kozlov, P. Martin, T.W. Tseng, D.W. Dawson, T.R. Donahue, A. Masamune, T. Shimosegawa, M.V. Apte, J.S. Wilson, B. Ng, S.L. Lau, J.E. Gunton, G.M. Wahl, T. Hunter, J.A. Drebin, P.J. O'Dwyer, C. Liddle, D.A. Tuveson, M. Downes, R.M. Evans, Vitamin D receptor-mediated stromal reprogramming suppresses pancreatitis and enhances pancreatic cancer therapy, Cell, 159 (2014) 80-93.

[18] I.S. Jamall, V.N. Finelli, S.S. Que Hee, A simple method to determine nanogram levels of 4-hydroxyproline in biological tissues, Anal Biochem, 112 (1981) 70-75.

[19] D. Debray, H. El Mourabit, F. Merabtene, L. Brot, D. Ulveling, Y. Chretien, D. Rainteau, I. Moszer, D. Wendum, H. Sokol, C. Housset, Diet-Induced Dysbiosis and Genetic Background Synergize With Cystic Fibrosis Transmembrane Conductance Regulator Deficiency to Promote Cholangiopathy in Mice, Hepatol Commun, 2 (2018) 1533-1549.

[20] A. Majdi, L. Aoudjehane, V. Ratziu, T. Islam, M.B. Afonso, F. Conti, T. Mestiri, M. Lagouge, F. Foufelle, F. Ballenghien, T. Ledent, M. Moldes, A. Cadoret, L. Fouassier, J.L. Delaunay, T. Ait-Slimane, G. Courtois, B. Feve, O. Scatton, C. Prip-Buus, C.M.P. Rodrigues, C. Housset, J. Gautheron, Inhibition of receptor-interacting protein kinase 1 improves experimental non-alcoholic fatty liver disease, Journal of hepatology, 72 (2020) 627-635.

[21] S. Basavappa, J. Middleton, A.W. Mangel, J.M. McGill, J.A. Cohn, J.G. Fitz, Cl- and K+ transport in human biliary cell lines, Gastroenterology, 104 (1993) 1796-1805.

[22] W. Stremmel, S. Staffer, R. Weiskirchen, Phosphatidylcholine Passes by Paracellular Transport to the Apical Side of the Polarized Biliary Tumor Cell Line Mz-ChA-1, International journal of molecular sciences, 20 (2019).

[23] S. Hohenester, L.M. Wenniger, C.C. Paulusma, S.J. van Vliet, D.M. Jefferson, R.P. Elferink, U. Beuers, A biliary HCO3- umbrella constitutes a protective mechanism against bile acid-induced injury in human cholangiocytes, Hepatology, 55 (2012) 173-183.

[24] L. Fouassier, P. Rosenberg, M. Mergey, B. Saubamea, A. Claperon, N. Kinnman, N. Chignard, G. Jacobsson-Ekman, B. Strandvik, C. Rey, V. Barbu, R. Hultcrantz, C. Housset, Ezrin-radixin-moesin-binding phosphoprotein (EBP50), an estrogen-inducible scaffold protein, contributes to biliary epithelial cell proliferation, The American journal of pathology, 174 (2009) 869-880.

[25] A. Baghdasaryan, T. Claudel, A. Kosters, J. Gumhold, D. Silbert, A. Thuringer, K. Leski, P. Fickert, S.J. Karpen, M. Trauner, Curcumin improves sclerosing cholangitis in Mdr2-/- mice by inhibition of cholangiocyte inflammatory response and portal myofibroblast proliferation, Gut, 59 (2010) 521-530.

[26] C.J. Soroka, D.N. Assis, L.S. Alrabadi, S. Roberts, L. Cusack, A.B. Jaffe, J.L. Boyer, Bile-Derived Organoids From Patients With Primary Sclerosing Cholangitis Recapitulate Their Inflammatory Immune Profile, Hepatology, 70 (2019) 871-882.

[27] N. Ding, R.T. Yu, N. Subramaniam, M.H. Sherman, C. Wilson, R. Rao, M. Leblanc, S. Coulter, M. He, C. Scott, S.L. Lau, A.R. Atkins, G.D. Barish, J.E. Gunton, C. Liddle,

M. Downes, R.M. Evans, A vitamin D receptor/SMAD genomic circuit gates hepatic fibrotic response, Cell, 153 (2013) 601-613.

[28] E.M. de Vries, M. de Krijger, M. Farkkila, J. Arola, P. Schirmacher, D. Gotthardt, B. Goeppert, P.J. Trivedi, G.M. Hirschfield, H. Ytting, B. Vainer, H.R. Buuren, K. Biermann, M.H. Harms, O. Chazouilleres, D. Wendum, A.D. Kemgang, R.W. Chapman, L.M. Wang, K.D. Williamson, A.S. Gouw, V. Paradis, C. Sempoux, U. Beuers, S.G. Hubscher, J. Verheij, C.Y. Ponsioen, Validation of the prognostic value of histologic scoring systems in primary sclerosing cholangitis: An international cohort study, Hepatology, 65 (2017) 907-919.

[29] S.Y. Cai, A. Mennone, C.J. Soroka, J.L. Boyer, Altered expression and function of canalicular transporters during early development of cholestatic liver injury in Abcb4-deficient mice, Am J Physiol Gastrointest Liver Physiol, 306 (2014) G670-676.

[30] N. Ikenaga, S.B. Liu, D.Y. Sverdlov, S. Yoshida, I. Nasser, Q. Ke, P.M. Kang, Y. Popov, A new Mdr2(-/-) mouse model of sclerosing cholangitis with rapid fibrosis progression, early-onset portal hypertension, and liver cancer, The American journal of pathology, 185 (2015) 325-334.

[31] W.S. Yang, H.W. Kim, J.M. Lee, N.J. Han, M.J. Lee, S.K. Park, 1,25-dihydroxyvitamin D3 causes ADAM10-dependent ectodomain shedding of tumor necrosis factor receptor 1 in vascular smooth muscle cells, Mol Pharmacol, 87 (2015) 533-542.

[32] W.S. Yang, H. Yu, J.J. Kim, M.J. Lee, S.K. Park, Vitamin D-induced ectodomain shedding of TNF receptor 1 as a nongenomic action: D3 vs D2 derivatives, J Steroid Biochem Mol Biol, 155 (2016) 18-25.

[33] K. Hochrath, S. Ehnert, C.L. Ackert-Bicknell, Y. Lau, A. Schmid, M. Krawczyk, J.G. Hengstler, J. Dunn, K. Hiththetiya, B. Rathkolb, K. Micklich, W. Hans, H. Fuchs, V. Gailus-Durner, E. Wolf, M.H. de Angelis, S. Dooley, B. Paigen, B. Wildemann, F. Lammert, A.K. Nussler, Modeling hepatic osteodystrophy in Abcb4 deficient mice, Bone, 55 (2013) 501-511.

[34] B. Dong, Y. Zhou, W. Wang, J. Scott, K. Kim, Z. Sun, Q. Guo, Y. Lu, N.M. Gonzales, H. Wu, S.M. Hartig, R.B. York, F. Yang, D.D. Moore, Vitamin D Receptor Activation in Liver Macrophages Ameliorates Hepatic Inflammation, Steatosis, and Insulin Resistance in Mice, Hepatology, 71 (2020) 1559-1574.

[35] J. Kong, Z. Zhang, M.W. Musch, G. Ning, J. Sun, J. Hart, M. Bissonnette, Y.C. Li, Novel role of the vitamin D receptor in maintaining the integrity of the intestinal mucosal barrier, Am J Physiol Gastrointest Liver Physiol, 294 (2008) G208-216.

[36] F.P. Reiter, L. Ye, F. Bosch, R. Wimmer, R. Artmann, A. Ziesch, V. Kanitz, D. Mayr, C.J. Steib, M. Trauner, I. Regel, A.L. Gerbes, J. Mayerle, S. Hohenester, E.N. de Toni, G. Denk, Antifibrotic effects of hypocalcemic vitamin D analogs in murine and human hepatic stellate cells and in the CCl4 mouse model, Laboratory investigation; a journal of technical methods and pathology, 99 (2019) 1906-1917.

[37] E. Wahsh, N. Abu-Elsaad, A. El-Karef, T. Ibrahim, The vitamin D receptor agonist, calcipotriol, modulates fibrogenic pathways mitigating liver fibrosis in-vivo: An experimental study, Eur J Pharmacol, 789 (2016) 362-369.

[38] X. Wang, G. Wang, J. Qu, Z. Yuan, R. Pan, K. Li, Calcipotriol Inhibits NLRP3 Signal Through YAP1 Activation to Alleviate Cholestatic Liver Injury and Fibrosis, Frontiers in pharmacology, 11 (2020) 200.

[39] F.P. Reiter, S. Hohenester, J.M. Nagel, R. Wimmer, R. Artmann, L. Wottke, M.C. Makeschin, D. Mayr, C. Rust, M. Trauner, G.U. Denk, 1,25-(OH)(2)-vitamin D(3) prevents activation of hepatic stellate cells in vitro and ameliorates inflammatory liver

damage but not fibrosis in the Abcb4(-/-) model, Biochem Biophys Res Commun, 459 (2015) 227-233.

[40] C. Tohda, T. Urano, M. Umezaki, I. Nemere, T. Kuboyama, Diosgenin is an exogenous activator of 1,25D(3)-MARRS/Pdia3/ERp57 and improves Alzheimer's disease pathologies in 5XFAD mice, Scientific reports, 2 (2012) 535.

[41] J. Chen, M. Doroudi, J. Cheung, A.L. Grozier, Z. Schwartz, B.D. Boyan, Plasma membrane Pdia3 and VDR interact to elicit rapid responses to 1alpha,25(OH)(2)D(3), Cell Signal, 25 (2013) 2362-2373.

[42] S. Petta, S. Grimaudo, C. Tripodo, D. Cabibi, M. Calvaruso, A. Di Cristina, C. Guarnotta, F.S. Macaluso, M.G. Minissale, G. Marchesini, A. Craxi, The hepatic expression of vitamin D receptor is inversely associated with the severity of liver damage in genotype 1 chronic hepatitis C patients, J Clin Endocrinol Metab, 100 (2015) 193-200.

[43] A. Beilfuss, J.P. Sowa, S. Sydor, M. Beste, L.P. Bechmann, M. Schlattjan, W.K. Syn, I. Wedemeyer, Z. Mathe, C. Jochum, G. Gerken, R.K. Gieseler, A. Canbay, Vitamin D counteracts fibrogenic TGF-beta signalling in human hepatic stellate cells both receptor-dependently and independently, Gut, 64 (2015) 791-799.

FIGURE LEGENDS

Figure 1. VDR ablation has a deleterious impact on the phenotype of *Abcb4* knockout mice.

Vdr^{-/-};Abcb4^{-/-} compared to *Vdr^{+/+};Abcb4^{-/-}* mice showed (A) a reduction of survival estimated by the Kaplan-Meier method (*n*=15 mice per group) and (B-D) more severe course of liver disease, as indicated by analyses at different time points of (B) liver weight and spleen weight to body weight ratios (*n*=8-14 mice per group); (C) hematoxylin and eosin-stained liver tissue sections (arrowheads point to onion-skin type fibrosis and fibrotic septa) and (D) plasma concentrations of aspartate aminotransferase (AST), alkaline phosphatase (ALP), total bilirubin and bile acids (*n*=5-10 mice per group). Bar graphs represent means ± SD; dashed lines represent the mean values in *n*=6 (8 weeks old) wildtype (WT) mice; *P<0.05; **P<0.01; ***P<0.001; ****P<0.0001 (Log-rank test for A; Mann-Whitney *U* test for B and D). Scale bars = 500 μm.

Figure. 2. VDR ablation aggravates cholangiopathy features in *Abcb4* knockout mice.

Vdr^{-/-};Abcb4^{-/-} compared to *Vdr^{+/+};Abcb4^{-/-}* mice showed more severe cholangiopathy as indicated by analyses at different time points of (A) ductular reaction assessed by cytokeratin 19 (CK19) immunostaining (*n*=6-7 mice per group), (B-C) hepatic inflammation assessed by (B) RT-qPCR of tumor necrosis factor α (*Tnfα*), vascular cell adhesion molecule 1 (*Vcam1*), C-C motif chemokine ligand (*Ccl*) *2*, *Ccl20*, *S100a8*, *S100a9*, matrix metalloproteinase 9 (*Mmp9*) (*n*=6-9 mice per group), expressed relative to a pool of hepatic mRNA from *n*=8 (8 weeks old) wildtype (WT) mice and (C) F4/80 immunostaining of macrophages (*n*=6-7 mice per group). (D) liver fibrosis assessed by Sirius red staining and hydroxyproline content (*n*=7-8 mice per group). Bar graphs represent means ± SD; dashed lines represent the mean values in *n*=6 (8 weeks old) WT

mice; *$P<0.05$; **$P<0.01$; ***$P<0.001$ (Mann-Whitney U test). Scale bars = 250 μm in A and C, and 500 μm in D.

Figure. 3. Calcipotriol treatment reverses the aggravation of cholangiopathy features elicited by the lack of VDR in *Abcb4* knockout mice.

Vdr$^{+/+}$;*Abcb4*$^{-/-}$ and *Vdr*$^{-/-}$;*Abcb4*$^{-/-}$ mice received intraperitoneal injections of calcipotriol (40 μg/kg) or vehicle, 3 times a week from the age of 4 weeks to 8 weeks, and upon sacrifice at 8 weeks, their liver phenotype was assessed by (A) Plasma concentrations of aspartate aminotransferase (AST), alkaline phosphatase (ALP), total bilirubin and bile acids (*n*=5-8 mice per group). (B) Cytokeratin 19 (CK19) immunostaining (*n*= 7-8 mice per group). (C) RT-qPCR analyses of the pro-inflammatory factors, tumor necrosis factor α (*Tnfα*), vascular cell adhesion molecule 1 (*Vcam1*), C-C motif chemokine ligand *(Ccl) 2*, *Ccl20*, *S100a8*, *S100a9* and matrix metalloproteinase 9 (*Mmp9*), in liver (*n*=7-8 mice per group), expressed relative to a pool of hepatic mRNA from 8 (8 weeks old) wildtype (WT) mice. (D) F4/80 immunostaining of macrophages (*n*=6-7 mice per group). (E) Sirius red staining and hydroxyproline content in liver (*n*=7-8 mice per group). Bar graphs represent means ± SD; dashed lines in A represent mean baseline values at the starting point of calcipotriol treatment in 4 weeks old *Vdr*$^{+/+}$;*Abcb4*$^{-/-}$ and *Vdr*$^{-/-}$;*Abcb4*$^{-/-}$ mice. *$P<0.05$ (Mann-Whitney U test). Scale bars = 250 μm in B and D, and 500 μm in E.

Figure 4. Protein disulfide-isomerase A3 (PDIA3) is overexpressed in the liver and cholangiocytes of *Abcb4* knockout mice lacking VDR.

PDIA3 expression was analyzed in (A-D) 8 weeks old mice (A-B) whole liver from *n*=6-9 per group by RT-qPCR and by immunoblot; (C) individual liver cell populations (*n*=1 mRNA pool from 6-8 mice) by RT-qPCR; In A and C, results are expressed relative to a pool of hepatic mRNA from *n*=8 wildtype (WT) mice); (D) in cholangiocytes (*n*=3 different mRNA pools from 3-4 mice) by RT-qPCR (results are expressed relative to a

pool of cholangiocyte mRNA from n=8 WT mice; numbers within bars represent Ct values); (E) in tissue sections of normal human liver or liver from a patient with PSC; representative images highlight PDIA3 expression at the plasma membrane of cholangiocytes, both in small and large bile ducts (arrows and inset). Bar graphs represent means ± SD; *P<0.05 (Kurskall-Wallis test followed by Dunn's multiple comparison); Hep, hepatocytes; Chol, cholangiocytes; HSC, hepatic stellate cells; LSEC, liver sinusoidal endothelial cells; KC, Kupffer cells. Scale bars = 10 μm.

Figure 5. The lack of VDR triggers a pro-inflammatory response in biliary epithelial cells that is counteracted by calcipotriol *via* PDIA3.

The expression of the proinflammatory factors, tumor necrosis factor α (TNFα), vascular cell adhesion molecule 1 (*VCAM1*), C-C motif chemokine ligand (CCL) 2, CCL20, S100A8, S100A9 and/or matrix metalloproteinase 9 (MMP9), was measured by RT-qPCR in the human biliary epithelial cells Mz-ChA-1, that were transfected with scramble siRNA, or *VDR* siRNA alone or combined with *PDIA3* siRNA, and 96 hours after transfection, analyzed in (A) basal conditions (n=8-10 independent experiments), or (B) incubated with vehicle or TNFα (10 ng/mL) with or without calcipotriol (100 nmol/L) for 24 hours (n=8 independent experiments). Bar graphs represent means ± SD; *P<0.05; **P<0.01 (paired Student t test for A; one-way ANOVA with Bonferroni post-hoc test for B). ND, not detected.

Figure 6. Long-term vitamin D supplementation reduces the severity of cholangiopathy features in Abcb4 knockout mice lacking VDR.

Vdr$^{+/+}$;*Abcb4*$^{-/-}$ and *Vdr*$^{-/-}$;*Abcb4*$^{-/-}$ mice were fed a regular or vitamin D (VD) supplemented diet after weaning, and upon sacrifice at 6 months, they underwent analyses of liver phenotype. (A) plasma concentrations of aspartate aminotransferase (AST), alkaline phosphatase (ALP), total bilirubin and bile acids (n=6-8 mice per group). (B)

Cytokeratin 19 (CK19) immunostaining (n=6-7 mice per group). (C) Sirius red staining and hydroxyproline content in liver (n= 7 mice per group). (D) Survival curves calculated by the Kaplan-Meier method in $Vdr^{+/+}$;$Abcb4^{-/-}$ and $Vdr^{-/-}$;$Abcb4^{-/-}$ mice, fed a regular or vitamin D (VD) supplemented diet (n=15 mice per group). Bar graphs represent means ± <u>SD</u>; *P<0.05; **P<0.01 (Mann-Whitney U test for A-C; Log-rank test for D). Scale bars = 250 μm and 500 μm in B and C, respectively.

Figure 1

Figure 2
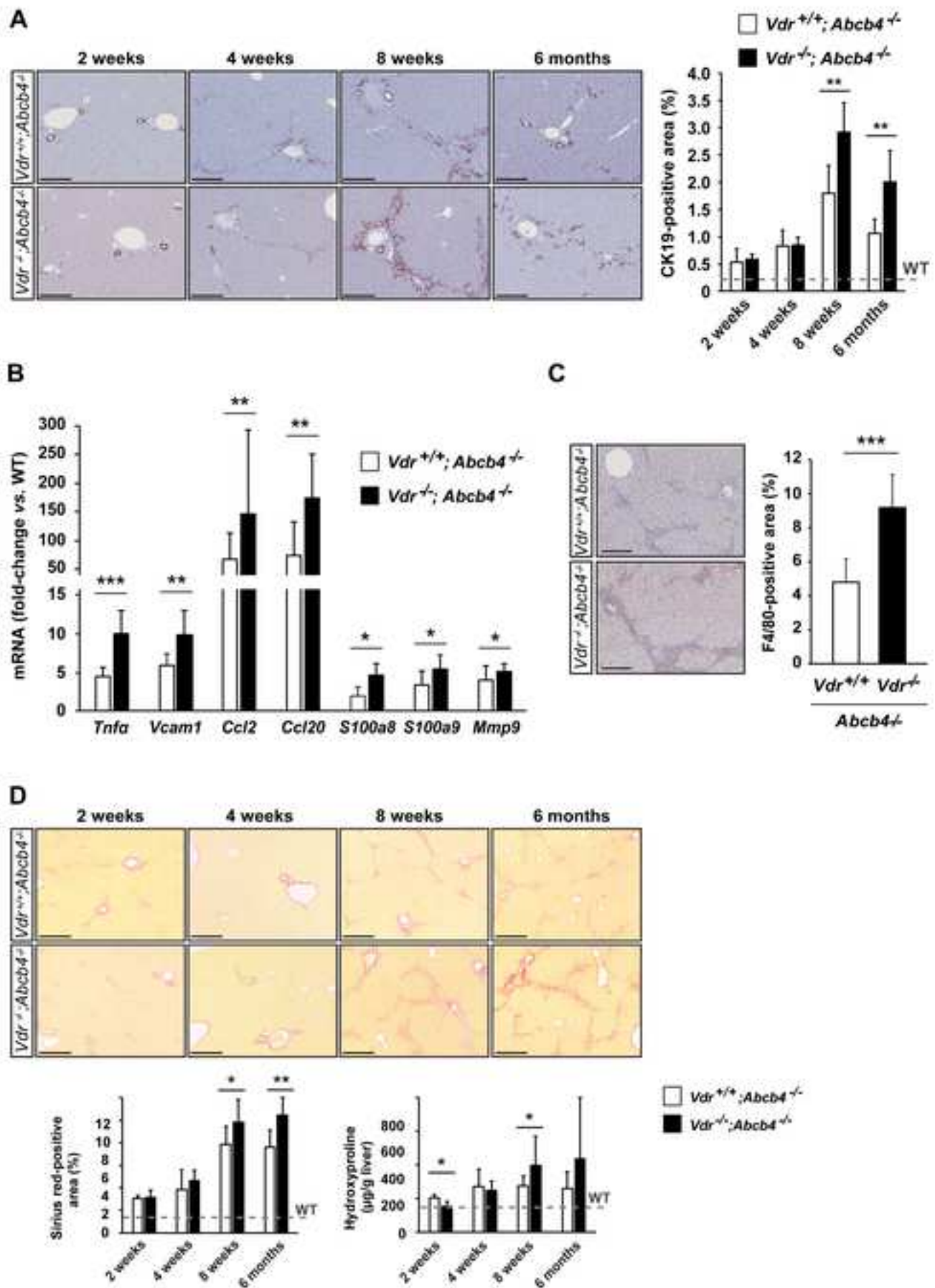
Figure 3
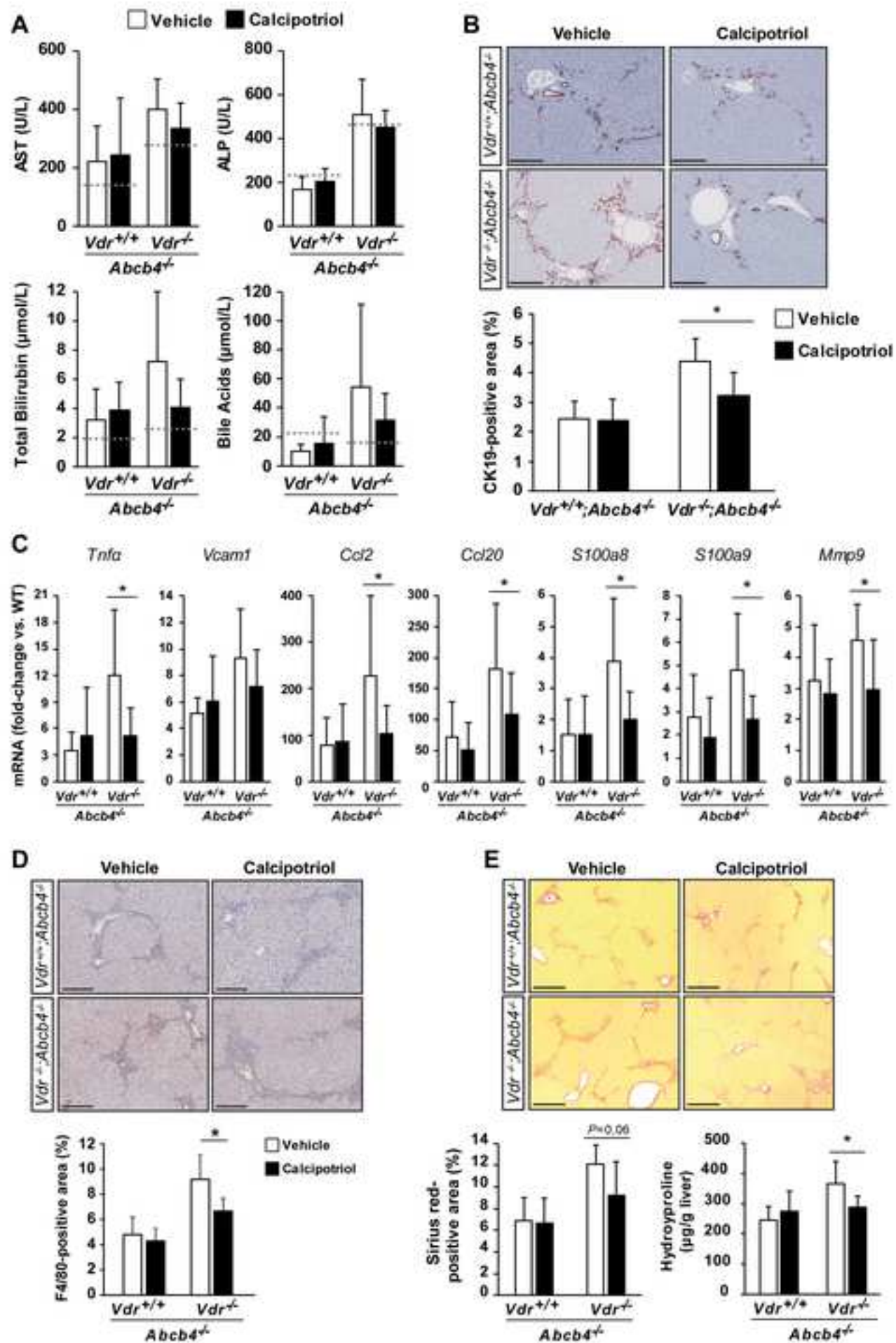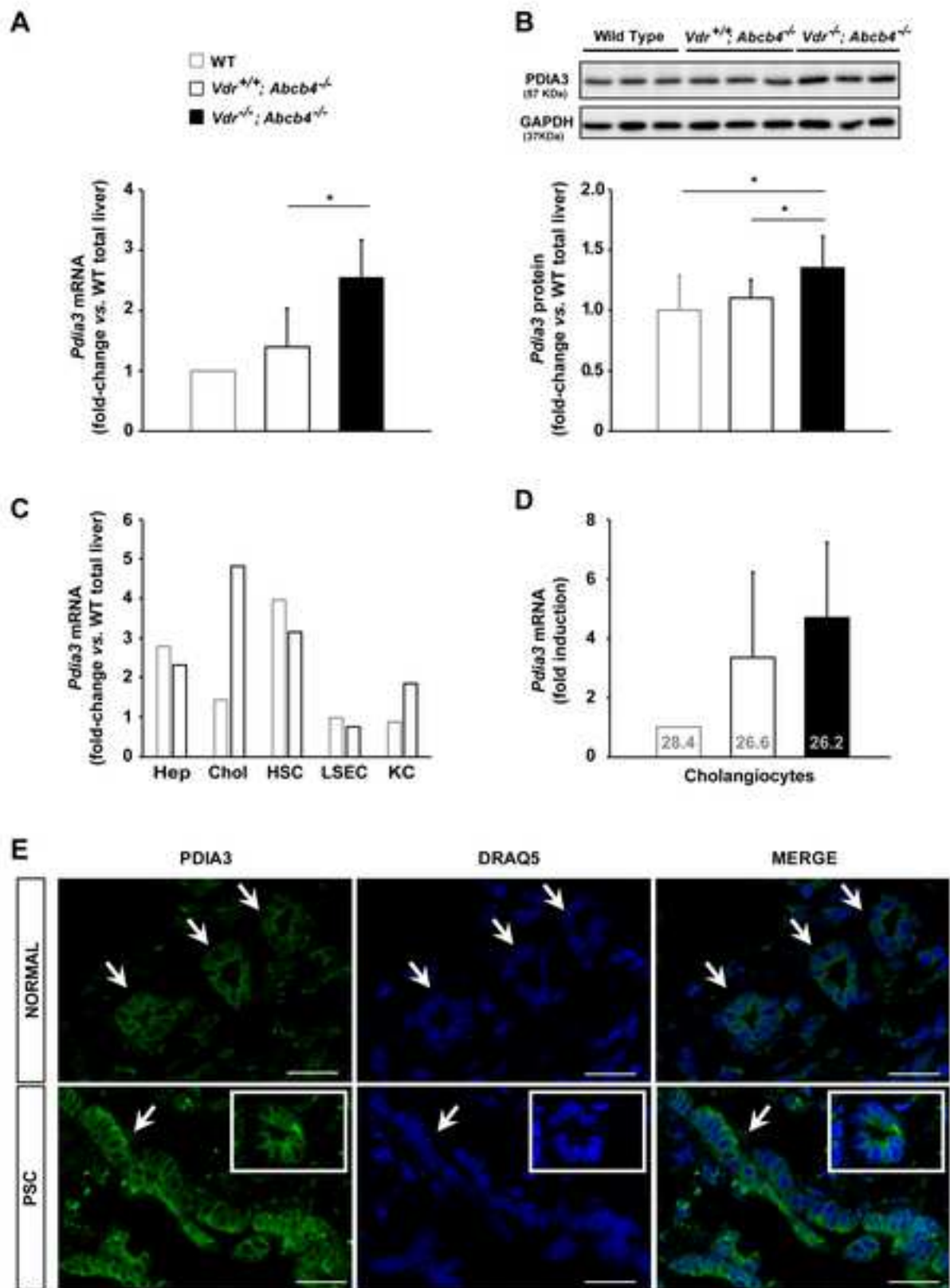
Figure 3
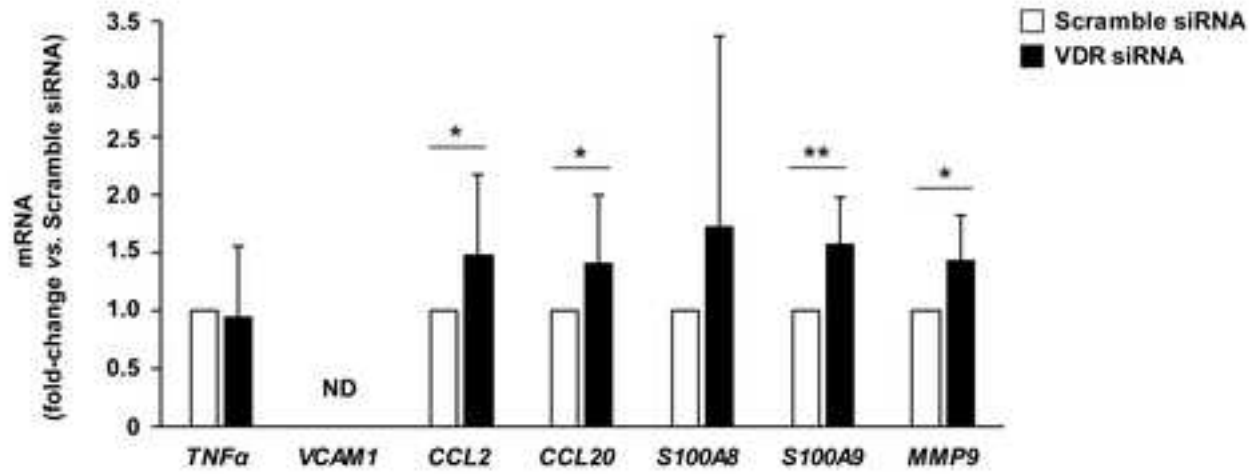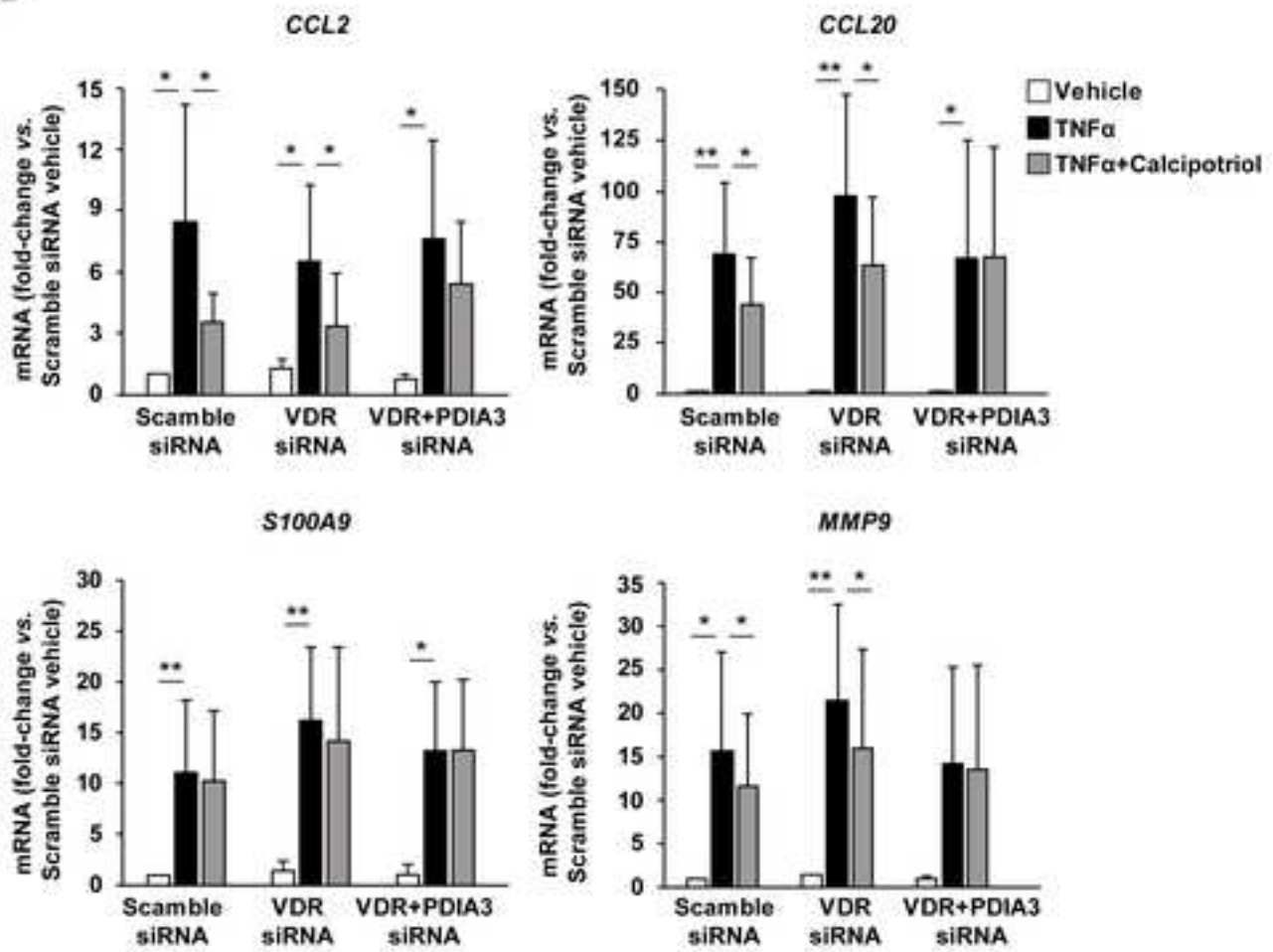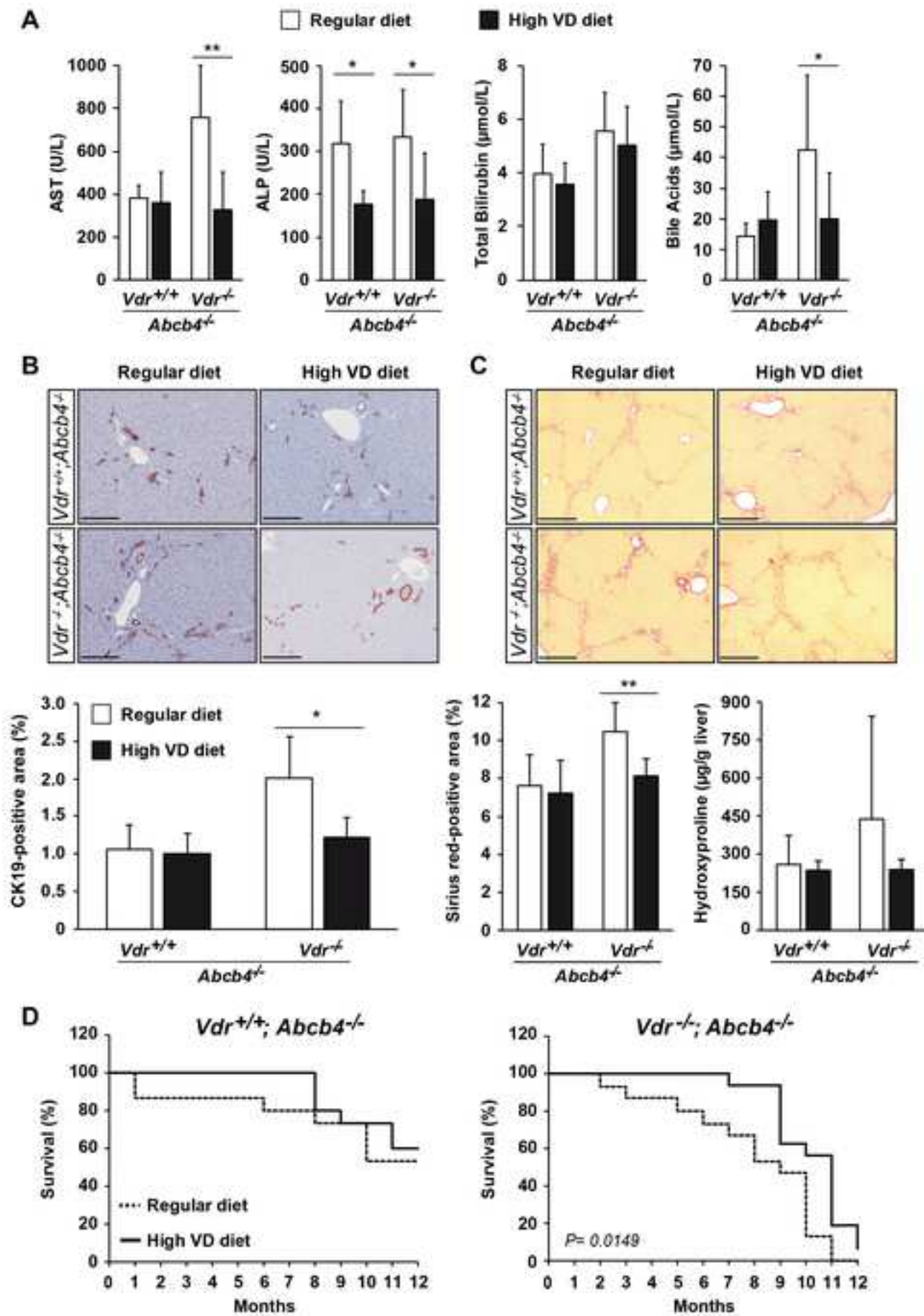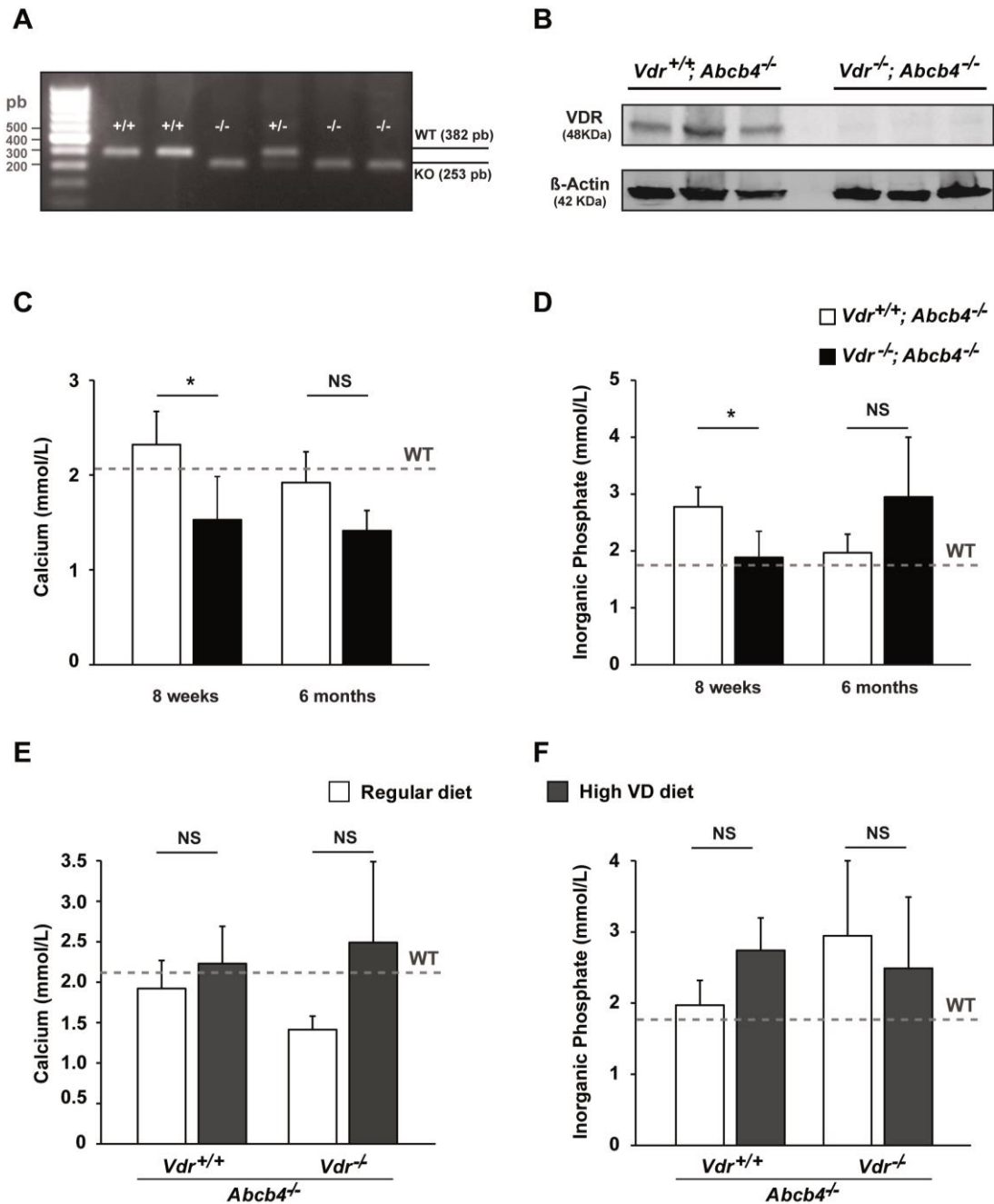
Figure 4

Figure 4

Figure 5

Figure 6

Cholangiopathy aggravation is caused by VDR ablation and alleviated by VDR-independent vitamin D signaling in ABCB4 knockout mice

Ester Gonzalez-Sanchez, Haquima El Mourabit, Marion Jager, Marie Clavel, Sophie Moog, Javier Vaquero, Tatiana Ledent, Axelle Cadoret, Jérémie Gautheron, Laura Fouassier, Dominique Wendum, Nicolas Chignard, Chantal Housset

Table of contents

Supplementary Figure S1. Characterization of $Vdr^{-/-}$; $Abcb4^{-/-}$ mice.

(A) *Vdr* genotype in animals generated by crossing $Vdr^{+/-}$;$Abcb4^{-/-}$ mice. (B) VDR expression assessed by immunoblot in colon from 8 weeks old $Vdr^{+/+}$;$Abcb4^{-/-}$ and $Vdr^{-/-}$;$Abcb4^{-/-}$ mice. (C-F) Plasma concentrations of calcium and phosphate in (C,D) 8 weeks and 6 months old $Vdr^{+/+}$;$Abcb4^{-/-}$ and $Vdr^{-/-}$;$Abcb4^{-/-}$ mice (*n*=2-4 mice per group) and (E,F) 6 months old $Vdr^{+/+}$;$Abcb4^{-/-}$ and $Vdr^{-/-}$;$Abcb4^{-/-}$ mice fed a regular or high vitamin D (VD) diet after weaning (*n*=2-4 mice per group). Bar graphs represent means ± SD, and dashed lines the mean value in 4 wildtype (WT) FVB/N mice ; *P<0.05; NS, not significant (Mann-Whitney *U* test).
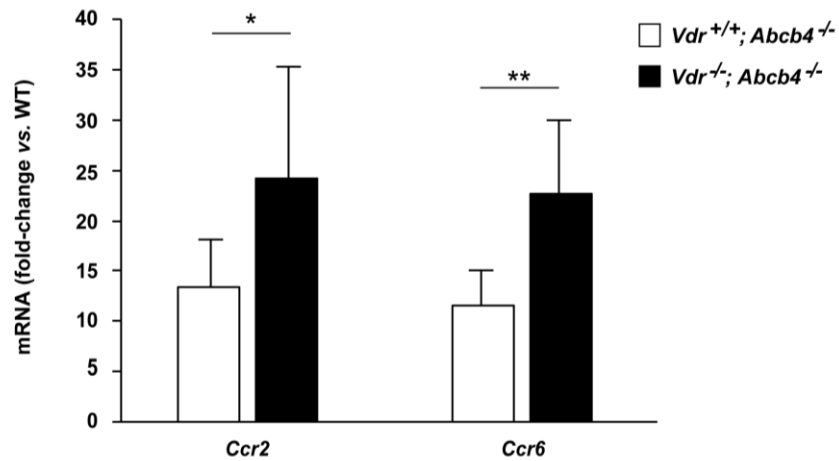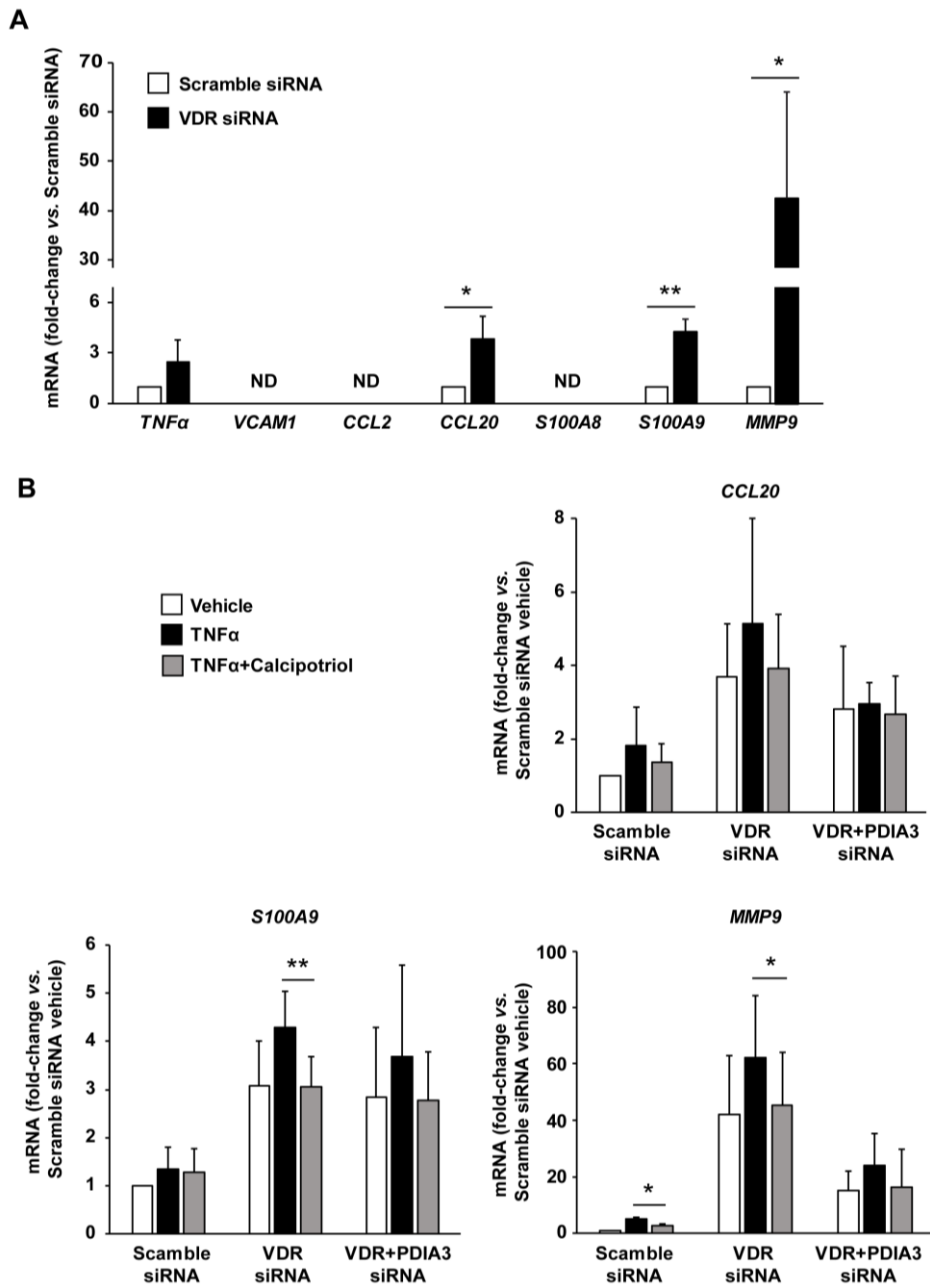
Supplementary Figure S2. Overexpression of chemokine receptors in the liver of *Vdr^{-/-};Abcb4^{-/-}* mice.

The expression of C-C motif chemokine receptor (*Ccr*)2 and *Ccr6* was analyzed in the liver of 8 weeks old *Vdr^{+/+};Abcb4^{-/-}* and *Vdr^{-/-};Abcb4^{-/-}* mice, by means of RT-qPCR. The mRNA levels are expressed relative to a pool of hepatic mRNA from 8 (8 weeks old) wildtype (WT) mice, and represent the means ± SD of 6-9 animals per group; *$P<0.05$; **$P<0.01$ (Mann-Whitney *U* test).
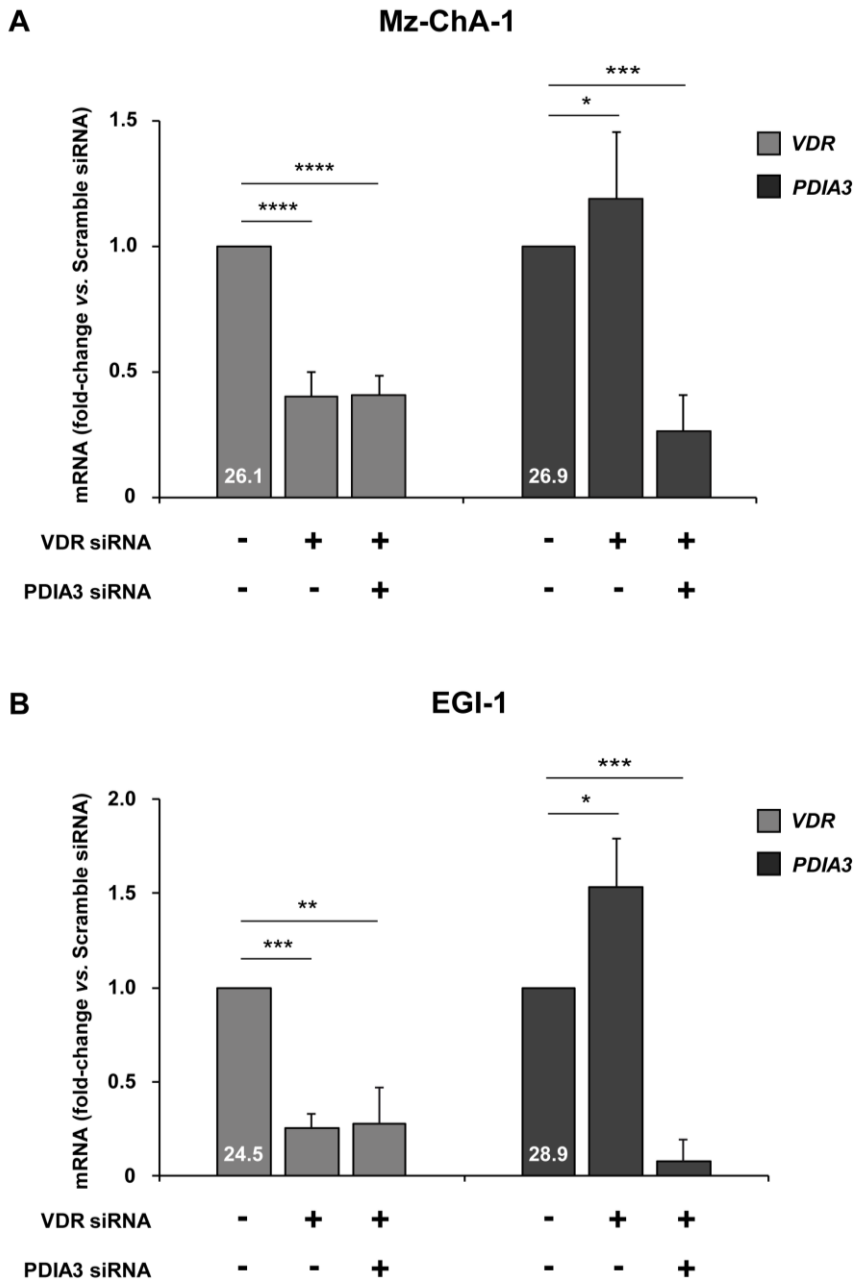
A   **Mz-ChA-1**

B   **EGI-1**

Supplementary Figure S3. VDR and PDIA3 silencing in biliary epithelial cells.

The human biliary epithelial cells, (A) Mz-ChA-1, and (B) EGI-1, were transfected with scramble siRNA, or VDR siRNA alone or combined with PDIA3 siRNA. Ninety-six hours after transfection, *VDR* and *PDIA3* expression was assessed by RT-qPCR. The mRNA levels are expressed relative to those in cells transfected with scramble siRNA, and represent the means ± SD of 8 experiments for MZ-Cha-1 and 4 experiments for EGI-1 (Ct values are indicated within bars); $*p<0.05$; $**p<0.01$; $***p<0.001$; $****$ $p<0.001$ (one way ANOVA with Bonferroni post-hoc test).

4

Supplementary Figure S4. The lack of VDR triggers a pro-inflammatory response in EGI-1 cells that is counteracted by calcipotriol *via* PDIA3.

The expression of the proinflammatory factors, tumor necrosis factor α (*TNFα*), vascular cell adhesion molecule 1 (*VCAM1*), C-C motif chemokine ligand (*CCL*) *2, CCL20, S100A8, S100A9* and/or matrix metalloproteinase 9 (*MMP9*), was measured by RT-qPCR in the human biliary epithelial cells EGI-1, that were transfected with scramble siRNA, or VDR siRNA alone or combined with PDIA3 siRNA, and 96 hours after transfection, (A) analyzed in basal conditions, or (B) incubated with vehicle or TNFα (10 ng/mL) with or without calcipotriol (100 nmol/L), for 24 hours. Bar graphs represent the means ± SD of 3 independent experiments; *$P<0.05$; **$P<0.01$ (paired Student *t* test in A; one way ANOVA with Bonferroni post-hoc test in B). ND, not detected.
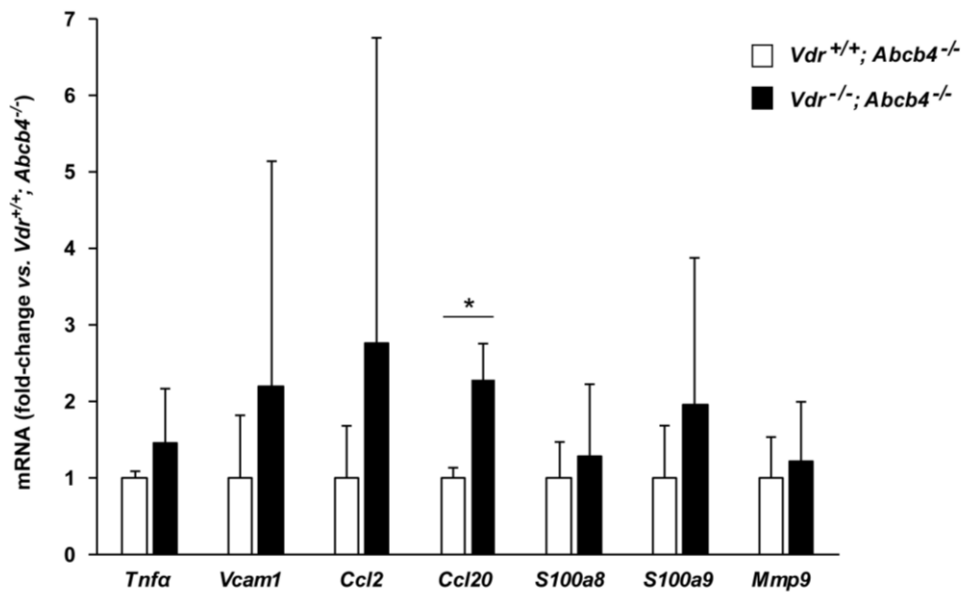
Supplementary Figure S5. VDR ablation triggers a pro-inflammatory response in cholangiocytes in *Abcb4* knockout mice.

The expression of the proinflammatory factors, tumor necrosis factor α (*Tnfα*), vascular cell adhesion molecule 1 (*Vcam1*), C-C motif chemokine ligand (*Ccl*) *2*, *Ccl20*, *S100a8*, *S100a9* and/or matrix metalloproteinase 9 (*Mmp9*), was measured by RT-qPCR in cholangiocytes isolated from 8 week-old *Vdr*$^{+/+}$;*Abcb4*$^{-/-}$ and *Vdr*$^{-/-}$;*Abcb4*$^{-/-}$ mice. (*n*= 3 different mRNA pools of cholangiocytes isolated from 3-4 animals). Bar graphs represent means ±SD; *$P<0.05$ (Mann-Whitney *U* test).
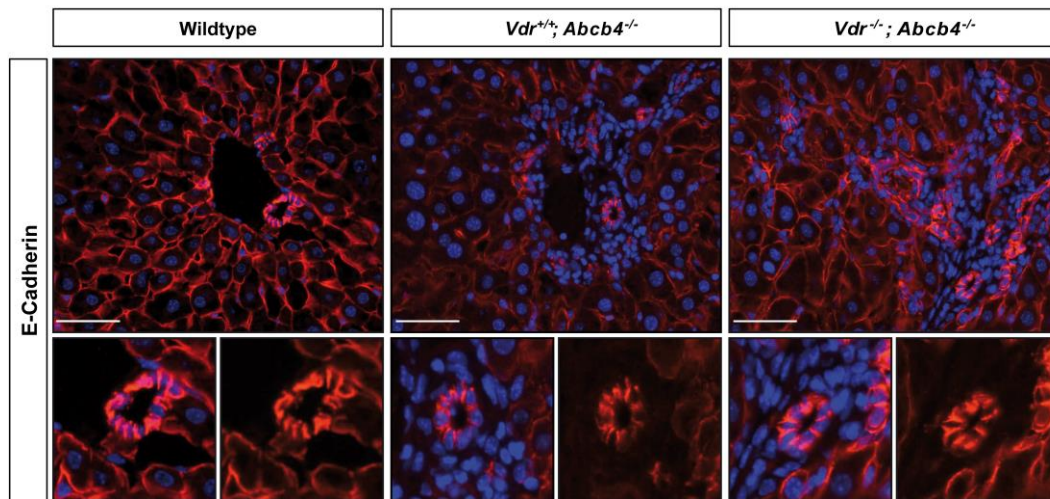
Supplementary Figure S6. Similar pattern of E-cadherin expression in the bile ducts of *Vdr*^{+/+};*Abcb4*^{-/-} and *Vdr*^{-/-};*Abcb4*^{-/-} mice.

Immunolabeling of the adherens junction protein, E-cadherin, was performed on liver tissue cryo-sections from 8 weeks old wildtype, $Vdr^{+/+}$;$Abcb4^{-/-}$ and $Vdr^{-/-}$;$Abcb4^{-/-}$ mice. Nuclear staining was performed, using DAPI. Tissue sections were scanned on a virtual slide scanner (Hamamatsu, Tokyo, Japan) 2.0 HT. Representative images of 6 to 9 animals per group are shown. Scale bars = 5 μm.

A

B
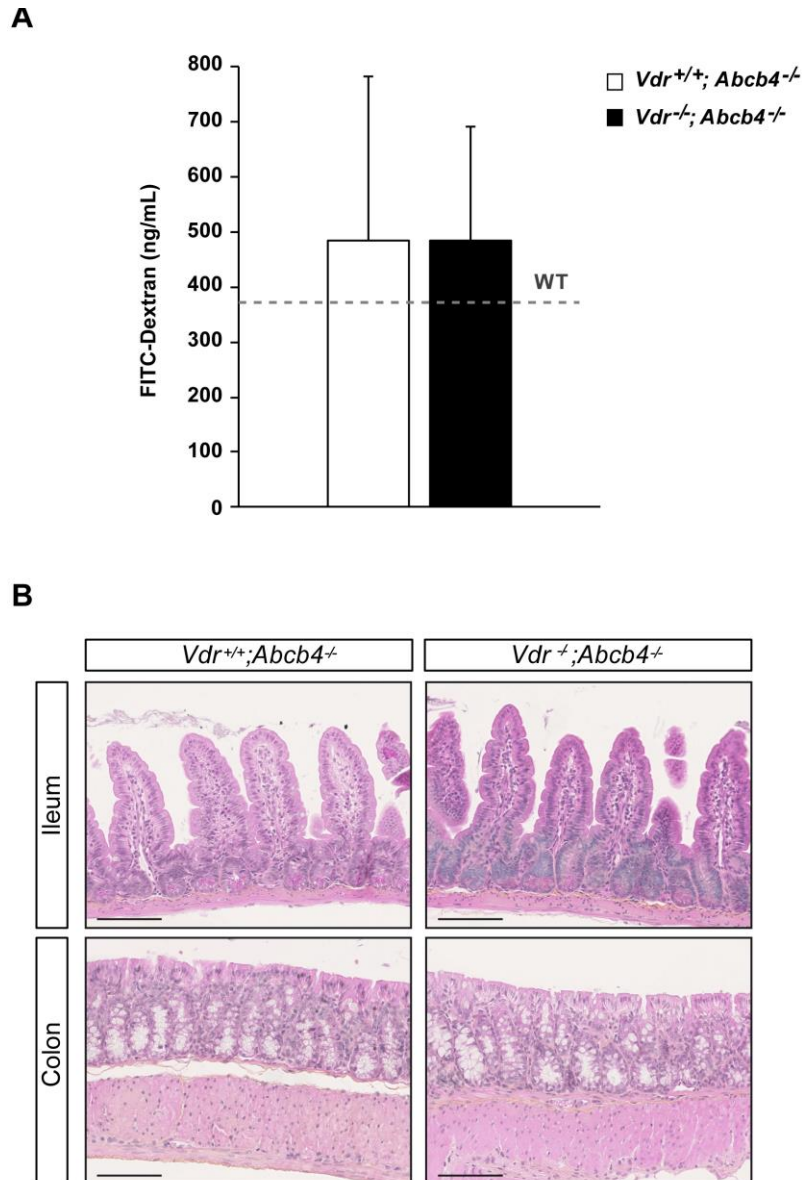
Supplementary Figure S7. Similar intestinal features in *Vdr$^{+/+}$;Abcb4$^{-/-}$* and *Vdr$^{-/-}$;Abcb4$^{-/-}$* mice.

(A) Intestinal permeability was assessed in 8-week old wildtype (WT), *Vdr$^{+/+}$;Abcb4$^{-/-}$* and *Vdr$^{-/-}$;Abcb4$^{-/-}$* mice, by fluorimetric dosage in plasma, 4 hours after administration of FITC-dextran 4.0 kDa by gavage. Bar graphs represent the means ± SD of 10 animals per group; the dashed line represent the mean value in 4 WT mice. (B) Representative images of hematoxylin and eosin-stained ileum and colon tissue sections in 8 weeks old wildtype *Vdr$^{+/+}$;Abcb4$^{-/-}$* and *Vdr$^{-/-}$;Abcb4$^{-/-}$* mice. Scale bars = 100 μm.

Supplementary Table S1. RT-qPCR primers sequences

Gene	Forward (5' > 3')	Reverse (5' > 3')	Access number
Mouse			
Tnfα	ATGAGCACAGAAAGCATGATC	TACAGGCTTGTCACTCGAATT	NM_013693.3; NM_001278601.1
Vcam1	TCTTACCTGTGCGCTGTGAC	ACTGGATCTTCAGGGAATGAGT	NM_011693.3
Ccl2	GCCTGCTGTTCACAGTTGC	CAGGTGAGTGGGGCGTTA	NM_011333
Ccl20	AACTGGGTGAAAAGGGCTGT	GTCCAATTCCATCCCAAAAA	NM_016960.2; NM_001159738.1
S100a8	TCCTTGCGATGGTGATAAAA	GGCCAGAAGCTCTGCTACTC	NM_013650.2
S100a9	AATGGTGGAAGCACAGTTGG	GCTCAGCTGATTGTCCTGGT	NM_001281852.1; NM_009114.3
Mmp9	CGTCGTGATCCCCACTTACT	AACACACAGGGTTTGCCTTC	NM_013599.4
Ccr2	GGCCACCACACCGTATGACTA	AGAGATGGCCAAGTTGAGCAG ATA G	NM_009915.2
Ccr6	CCTACTTTGGAACGGATGATTATGAC	GGATCTGGCTTTCTTGTAGAAGGC A	NM_009835.4; NM_001190333.1 NM_001190334.1 NM_001190335.1; NM_001190336.1; NM_001190337.1 NM_001190338.1
Pdia3	CCAATGATGTGCCTTCTC	TGTGCCTTCTTCTTCTTC	NM_007952.2
Hprt1	TCAGTCAACGGGGGACATAA	TGCTTAACCAGGGAAAGCAAA	NM_013556.2
Human			
TNFα	CTCTCTCTAATCAGCCCTCT	AGCTGGTTATCTCTCAGCTC	NM_000594.4
VCAM1	AACAAAGGCAGAGTACGCAAA	TCATATTCACAGAACTGCCTTCC	NM_001078.4; NM_080682.2; NM_001199834.1
CCL2	CAGCCAGATGCAATCAATGCC	TGGAATCCTGAACCCACTTCT	NM_002982.4
CCL20	CTGTGACATCAATGCTATCATCTTTCA	CTTGGGCTATGTCCAATTCCATTCC	NM_004591.3; NM_001130046.2
S100A8	GAGACCGAGTGTCCTCAGTATATC	ACGCCCATCTTTATCACCAGAATGAGG	NM_001319196.1; NM_001319197.1; NM_001319198.1; NM_002964.5; NM_001319201.1
S100A9	ACGCAACATAGAGACCATCATC	GACCTTTTCATTCTTATTCTCCTTCTT	NM_002965.4
MMP9	ACCTCGAACTTTGACAGCGACA	GATGCCATTCACGTCGTCCTTA	NM_004994.3
PDIA3	CCAATGATGTGCCTTCTC	TGTGCCTTCTTCTTCTTC	NM_005313.5
VDR	ATCGGCATGATGAAGGAGTT	ATCGGCATGATGAAGGAGTT	NM_001364085.1; NM_001364085.1; NM_001017536.
GAPDH	AGCCACATCGCTCAGACAC	GCCCAATACGACCAAATCC	NM_002046.7; NM_001289745.3; NM_001289746.2; NM_001357943.2

TNFα, tumor necrosis factor α; *VCAM1*, vascular cell adhesion molecule 1; *CCL2*, C-C motif chemokine ligand 2; *CCL20*, C-C motif chemokine ligand 20; *MMP9*, matrix metalloproteinase 9; *CCR2*, C-C motif chemokine receptor 2; *CCR6*; C-C motif chemokine receptor 6; *PDIA3*, protein disulfide-isomerase A3; *HPRT1*, hypoxanthine phosphoribosyltransferase 1; *VDR*, vitamin D receptor; *GAPDH*, glyceraldehyde 3-phosphate dehydrogenase.

Supplementary Table S2. Histological scoring of liver damage in _Vdr$^{+/+}$;Abcb4$^{-/-}$_ and _Vdr$^{-/-}$;Abcb4$^{-/-}$_ mice.

	2 weeks		4 weeks		8 weeks		6 months	
	Vdr$^{+/+}$;Abcb4$^{-/-}$ n=5	_Vdr$^{-/-}$;Abcb4$^{-/-}$_ n=5	_Vdr$^{+/+}$;Abcb4$^{-/-}$_ n=5	_Vdr$^{-/-}$;Abcb4$^{-/-}$_ n=5	_Vdr$^{+/+}$;Abcb4$^{-/-}$_ n=6	_Vdr$^{-/-}$;Abcb4$^{-/-}$_ n=6	_Vdr$^{+/+}$;Abcb4$^{-/-}$_ n=5	_Vdr$^{-/-}$;Abcb4$^{-/-}$_ n=5
Cholangitis activity								
0	2	0	1	0	1	1	3	0
1	1	3	2	2	2	0	1	1
2	2	0	0	1	0	1	0	0
3	0	2	2	2	3	4	1	3
Hepatitis activity								
0	5	5	3	3	5	5	5	5
1	0	0	2	2	0	0	0	0
2	0	0	0	0	0	0	0	0
3	0	0	0	0	0	0	0	0
Fibrosis stage								
0	1	1	2	1	0	0	0	0
1	4	3	2	4	3	0	5	4
2	0	1	1	0	3	6	0	1
3	0	0	0	0	0	0	0	0
Bile duct loss								
0	5	5	5	5	5	5	5	4
1	0	0	0	0	0	0	0	0
2	0	0	0	0	0	0	0	0
3	0	0	0	0	0	0	0	1

Histological analysis was performed using an adaptation (described below) of Nakanuma scoring. Data represent the number of animals classified for each item on a 0-3 scale.

SUPPLEMENTARY MATERIALS AND METHODS

Mouse genotyping

$Vdr^{+/+};Abcb4^{-/-}$ and $Vdr^{-/-};Abcb4^{-/-}$ genotypes were assessed by Polymerase chain reaction (PCR). Briefly, total DNA was harvested from distal phalanx or tail biopsy using Direct PCR Lysis reagent (Viagen Biotech, Los Angeles, CA, USA) and proteinase K (Sigma-Aldrich, Saint-Louis, MO, USA). PCR was performed using specific primers for Vdr (wildtype 5'-CTCCATCCCCATGTGTCTTT-3', common 5'-TTCTTCAGTGGCCAGCTCTT-3', mutant 5'-CTAAAGCGCATGCTCCAGAC-3'), and DreamTaq Green DNA (Thermo Fischer Scientific, Walthman, MA, USA). PCR conditions were as follows: Pre-denaturation at 95°C for 5 min; followed by 35 cycles of 94°C for 30 sec, 60°C for 30 sec and 72°C for 30 sec, and a final extension step at 72°C for 10 min. PCR products were analyzed in 1.2% agarose gels.

Histological scoring

Hematoxylin and eosin-stained liver tissue sections were blindly analyzed by a senior pathologist expert in liver histopathology, D.W. following Nakamuna scoring (1). The following histopathologic features were assessed semi-quantitatively on a 0-3 scale: cholangitis activity, hepatitis activity, fibrosis stage and bile duct loss. Due to the specific characteristics of liver damage in $Abcb4^{-/-}$ mice, grading criteria for cholangitis activity were adapted as follows: grade 0: no activity; grade 1: one bile duct with polymorphonuclear cells infiltrate; grade 2: 2 or more bile ducts with polymorphonuclear cells infiltrate; grade 3: presence of fibro-obliterative cholangitis.

Immunofluorescence of E-cadherin

Liver tissue samples were collected from wildtype, $Vdr^{+/+};Abcb4^{-/-}$ and $Vdr^{-/-};Abcb4^{-/-}$ mice at the age of 8 weeks, snap-frozen in liquid nitrogen and stored at -80°C in OCT. Liver tissue cryosections (4-μm-thick) were fixed in paraformaldehyde (PFA) 4%, and incubated in PBS containing 3% bovine serum albumin (BSA) to block unspecific

binding, and 20 μmol/L Triton X to permeabilize tissue. Thereafter, sections were incubated with an antibody raised against E-cadherin (#13-1900, Thermo Fischer Scientific, Walthman, MA, USA) diluted 1/1000 in PBS containing 3% BSA and 20 μmol/L Triton X, overnight at 4°C. Sections were then incubated with a secondary anti-rat antibody coupled to Cyanine3 (#A10522, Invitrogen/Thermo Fischer Scientific) diluted 1/200 in PBS containing 3% BSA and 20 μmol/L Triton X, at room temperature for one hour. Nuclear staining was performed, using DAPI (Thermo Fisher Scientific) at 1/3000, for 5 min at room temperature. Tissue sections were scanned on a virtual slide scanner (Hamamatsu, Tokyo, Japan) 2.0 HT.

Intestinal permeability assay

Fluorescein isothiocyanate conjugated dextran (FITC-dextran 4.0 kDa, Sigma-Aldrich, Saint-Louis, MO, USA) dissolved in PBS at a concentration of 100 mg/mL was administered to mice (5 mL/kg body weight) by oral gavage. Four hours later, mice were sacrificed under isoflurane anesthesia. Blood samples were collected from inferior vena cava and immediately stored at 4°C in the dark. Concentrations of FITC-dextran in plasma were determined on a spectrophotofluorimeter (Tecan Infinite M200, Männedorf, Switzerland) at an excitation wavelength of 485 nm and an emission wavelength of 528 nm using standard serially diluted FITC-dextran (0, 62.5, 125, 250, 500, 1,000, 2,000, 4,000 ng/mL). To note, bilirubin has a similar emission wavelength as FITC-dextran and may interfere with this method in case of hyperbilirubinemia. To circumvent this potential interference, retroorbital blood was collected from the animals immediately before FITC-dextran administration, and the plasma used to determine background.

REFERENCES

1. de Vries EM, de Krijger M, Farkkila M, Arola J, Schirmacher P, Gotthardt D, et al. Validation of the prognostic value of histologic scoring systems in primary sclerosing cholangitis: An international cohort study. Hepatology. 2017;65(3):907-19.
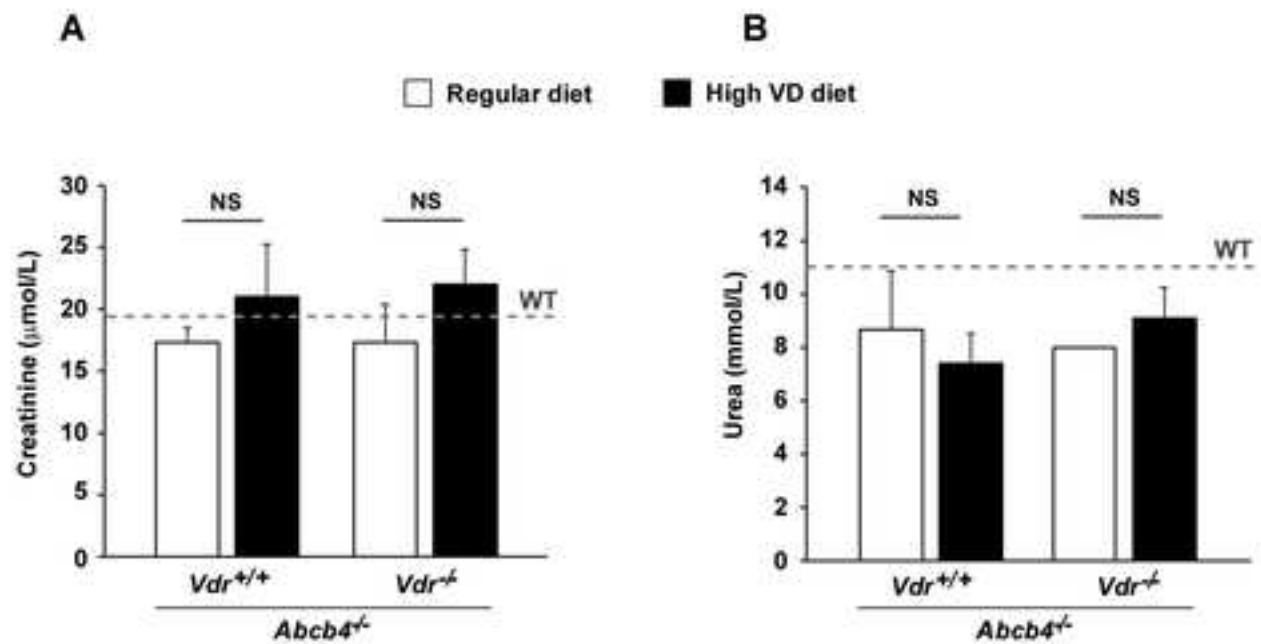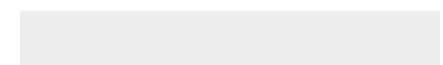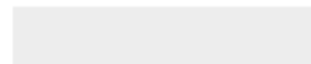
A

B

☐ Regular diet ■ High VD diet

Figure 1 for review purpose

*Declaration of Interest Statement

Click here to access/download
Declaration of Interest Statement
5.Gonzalez-Sanchez declaration-of-competing-interests
1.docx

CRediT authorship contribution statement: N.C., C.H. Conceptualization and Supervision ; E.G-S., H.E.M, M.J., M.C., Investigation and Formal analysis; T.L. Resources; S.M., Investigation; E.G-S., J.V., D.W., N.C., C.H. Methodology and Data Curation; E.G-S., N.C., C.H. Writing-Original Draft and -Review&Editing; J.V., H.E.M., J.G., A.C., L.F. Writing- Review&Editing; C.H. and E.G-S Project administration and Funding adquisition.